Research Square

Preprints are preliminary reports that have not undergone peer review.
They should not be considered conclusive, used to inform clinical practice,
or referenced by the media as validated information.

Understanding the Physiological Functions of the Host Xenobiotic-sensing Nuclear Receptors PXR and CAR on the Gut Microbiome using Genetically Modified Mice

Mallory Little
University of Washington
Moumita Dutta
University of Washington
Hao Li
Einstein College of Medicine
Adam Matson
University of Connecticut Official Bookstore
Xiaojian Shi
Arizona State University
Haiwei Gu
Arizona State University
Sridhar Mani
Hospital Israelita Albert Einstein
Julia Yue Cui (juliacui@uw.edu)
University of Washington https://orcid.org/0000-0002-8564-1784

Research

Keywords: PXR, CAR, gut microbiome, bile acids, cytokines

Posted Date: June 29th, 2020

DOI: https://doi.org/10.21203/rs.3.rs-36593/v1

License: This work is licensed under a Creative Commons Attribution 4.0 International License.
Read Full License

Version of Record: A version of this preprint was published at Acta Pharmaceutica Sinica B on July 1st, 2021. See the published version at https://doi.org/10.1016/j.apsb.2021.07.022.

Abstract

Background: Pharmacological activation of the host xenobiotic-sensing nuclear receptors pregnane X receptor (PXR) and constitutive androstane receptor (CAR) is well-known to increase drug metabolism and reduce inflammation. Little is known regarding the physiological functions of PXR and CAR on the gut microbiome, which is an important regulator for the host immune surveillance and bile acid (BA) metabolism. We examined the gut microbiome composition and BA metabolites in high vs. low PXR/CAR-expressing mice, and in mice that are deficient in PXR, CAR, or both, at two developmental ages. We also utilized humanized PXR transgenic (hPXR-TG) mice to compare the species-specific effect of PXR on the gut microbiome.

Results: We discovered bivalent hormetic functions of PXR and CAR in modulating the richness of the gut microbiome and inflammatory biomarkers: the high PXR/CAR expressers had higher microbial richness, pro-inflammatory bacteria (distinct taxa in *Helicobacteraceae* and *Helicobacter*), and fecal pro-inflammatory cytokines, suggesting higher immune surveillance to prevent the colonization of harmful bacteria. Interestingly, the absence of PXR or CAR also increased the microbial richness, and absence of both receptors synergistically increased the microbial richness. PXR and CAR deficiency increased the pro-inflammatory bacteria (*Helicobacteraceae* and *Helicobacter*). Most notably, deficiency in both PXR and CAR markedly increased the relative abundance of *Lactobacillus*, which is capable of bile salt hydrolase (BSH) activity. This corresponded to a decrease in major primary taurine-conjugated bile acids (BAs) in feces, which may lead to higher internal burden of taurine and unconjugated BAs, both of which are linked to inflammation, oxidative stress, and cytotoxicity. hPXR-TG mice had a distinct microbial profile as compared to wild-type mice, including a higher representation *of Prevotella*. hPXR-TG mice also had higher 12-OH BAs but lower 6-OH BAs, suggesting PXR's species-specific role in modulating host hepatic BA synthesis.

Conclusions: This study is the first to show that the host PXR and CAR profoundly influence the composition of the gut microbiome and its BA metabolites, with a bivalent hormetic relationship between PXR/CAR levels and microbial richness, unveiling the involvement of PXR/CAR-microbiome interactions in host immune surveillance and BA metabolism.

Background

The gut microbiome has a variety of effects on the intermediary metabolism of the host. One of the important functions of the gut microbiome is bile acid (BA) metabolism. In humans, primary BAs are synthesized from cholesterol in the liver, and are then conjugated with taurine (T) or glycine. In mice, T-conjugated BAs are predominant. In the intestine, bacteria can perform deconjugation, dehydroxylation, and epimerization reactions, generating more hydrophobic and thus more toxic BA profiles [5]. The microbial enzymes bile salt hydrolase and bile acid 7α-dehydroxylase catalyze BA deconjugation and secondary BA synthesis reactions, respectively [6]. Specific secondary BAs are more potent activators of the host Takeda G-protein-coupled receptor 5 (TGR-5) than primary BAs, and this can promote

thermogenesis and energy expenditure of the host [7]. At exceedingly high concentrations, unconjugated secondary BAs are considered more toxic than primary BAs and are implicated in cholestatic liver injury, inflammation, and cancer [8]. Specifically, unconjugated BAs (both primary and secondary) produce a more prominent increase in pro-inflammatory cytokines from hepatocytes during cholestatic liver injury [9]. Microbially-derived BAs are also known to contribute to inflammatory bowel disease (IBD) [10] and host immune surveillance by directly modulating the balance of T_H17 and T_{reg} cells [11]. This highlights the importance of gut microbiome and BAs on immune surveillance.

Gut microbiota also contribute to xenobiotic metabolism. For example, *Eggerthella lenta* contains cardiac glycoside operons (Cprs) that inactivate the cardiac glycoside digoxin [12]. Furthermore, it has been shown that co-administration of the antibiotic rifaximin with non-steroidal anti-inflammatory drugs (NSAIDs) ameliorates bacteria-induced enteropathy [13]. The gut microbiome can also modulate host xenobiotic metabolism through indirect mechanisms. For example, the absence of gut microbiota in mice alters the expression of xenobiotic-processing genes, such as those for cytochrome P450 enzymes and other phase I oxidases [14]. The absence of gut microbiota in mice alters the host metabolism of polybrominated diphenyl ethers (PBDEs), and modulates the PBDE-mediated differential regulation of xenobiotic-processing genes [15]. Therefore, the gut microbiome is an important direct and indirect regulator of host xenobiotic biotransformation pathways.

The well-known host xenobiotic-sensing nuclear receptors PXR and CAR are highly expressed in the liver and intestine. Upon ligand activation, PXR and CAR up-regulate certain drug-metabolizing enzymes and efflux transporters as a compensatory mechanism against xenobiotic insult [16, 17]. PXR and CAR share many target genes, such as the drug-metabolizing enzyme cytochrome P450 3A4 (CYP3A4) in humans [18]. PXR and CAR are known as promiscuous nuclear receptors because a wide variety of ligands can attach to their ligand-binding domains and induce gene transcription [20]. For example, PXR and CAR are both activated by the antifungal voriconazole and coordinate its metabolism [21]. PXR and CAR are also activated by environmental chemicals such as specific congeners of the PBDE flame retardants and non-coplanar polychlorinated biphenyls (PCBs) [22, 23]. In addition to environmental chemicals and pharmaceuticals, PXR and CAR can be activated by endogenous ligands such as steroids and BAs [24]. Several herbal drugs activate PXR and CAR [116, 117]. They are involved in drug-drug and drug-food interactions as well as human diseases such as inflammatory bowel disease (IBD) and cholestasis [25]. A wide variety of bacterial metabolites in the colonic lumen activate PXR and CAR, such as the tryptophan metabolite indole-3-propionic acid (IPA) and the secondary BAs deoxycholic acid (DCA) and lithocholic acid (LCA) [26]. It is theorized that these metabolites can bind to these nuclear receptors [27]. In livers of germ-free mice (GF), the prototypical PXR-target genes Cyp3a11 and Cyp3a44 were down-regulated compared to conventional (CV) mice with healthy intestinal microbiota. This down-regulation purportedly occurs because of reduced PXR-activation due to decreased microbial metabolite PXR ligands; however, this same study reported an increase in the mRNA of all transcription factors in livers of GF mice [28]. This relationship has been explored in another study where specific-pathogen-free (SPF) mice had higher cytochrome P450 isozyme expression with accompanying higher PXR and CAR expression than GF mice,

due to increased LCA [29]. Therefore, the presence of the gut microbiome affects the expression of PXR- and CAR-target genes, the receptors themselves, and the activity of PXR and CAR through modulating their activators.

Recent studies unveiled that PXR and CAR have anti-inflammatory functions. For example, pharmacological activation of PXR can play an anti-inflammatory role in the prevention of inflammatory bowel disease (IBD) by inhibiting the NF-κB transcription factor [30], as well as NF-κB-targeted pro-inflammatory response genes [25]. The activation of PXR via the microbial metabolite IPA, which is produced from *Clostridium sporogenes*, decreases intestinal permeability and maintains gut barrier functions [24]. PXR activation also inhibits inflammation by inhibiting the toll-like receptor 4 (TLR4) pathway, thus preventing the overproduction of cytokines. Inhibition of the TLR4 pathway results in resistance to *Listeria monocytogenes* infection compared to PXR-null mice [31]. PXR inhibits the TLR4 pathway by decreasing the stability of TLR4 mRNA and may also repress TLR4 gene transcription [32, 33]. This TLR4 up-regulation due to PXR deficiency can also cause leaky gut physiology [34], which can be resolved by PXR activation via microbial metabolites as previously described [35]. Additionally, PXR has been recognized for its role in energy homeostasis and glucose metabolism and is correlated with obesity [36]. Interestingly, CAR is negatively correlated with obesity and has been shown to improve insulin sensitivity [37]. Activation of CAR by environmental chemicals has been associated with rodent liver tumor formation, non-alcoholic fatty liver disease, as well as drug-interactions due to the up-regulation of Cyp3a enzymes [32, 38]. Polymorphisms can affect the function of PXR and CAR as well; for example, a single-nucleotide polymorphism (SNP) in PXR decreases risk for anti-tuberculosis drug-induced hepatotoxicity [39].

Pharmacological and toxicological exposures can affect the composition of the gut microbiome. Treatment with the non-steroidal anti-inflammatory drug (NSAID) indomethacin increased bacteria in the *S24-7* family compared to co-treatment with the microbial metabolite indole, which increased members of the *Clostridiales* order instead. Notably, co-treatment with indole reduced inflammation and intestinal mucosal damage [47], possibly through a PXR-mediated mechanism. Indole-3 propionic acid (IPA) activates mouse PXR, leading to the down-regulation of the TLR pathway and pro-inflammatory tumor necrosis factor α (TNFα) [34]. Mice treated with statins gained weight, had increased members of the *S24-7* family, had up-regulation of PXR-target genes, reduced butyrate, and increased DCA. These effects of statins were found to be PXR-dependent [48]. In mice, pharmacological activation of PXR and CAR by their prototypical ligands PCN and TCPOBOP affects the composition of the gut microbiome in part by down-regulating certain BA-metabolizing bacteria in the intestine [49]. Furthermore, mice orally-gavaged with PBDEs, which are PXR and CAR activators, had increased *Akkermansia muciniphila* and *Allobaculum* spp., as well as unconjugated secondary BAs [22]. In another study, mice dosed with PCBs, which can also activate PXR and CAR, had increased *A. muciniphila*, *Clostridium scindens*, *Enterococcus* sp., and *Prevotella* sp. as well as serum BAs [50]. In summary, pharmacological and toxicological activation of PXR and CAR can alter the composition of the gut microbiome and the production of distinct microbial metabolites.

While a wealth of literature has demonstrated that the gut microbiome affects PXR and CAR through microbial metabolites, and that pharmacological and toxicological PXR activation affects the composition of the gut microbiome, no studies have been conducted examining the physiological functions of PXR and CAR on the gut microbiome. Therefore, this study aims to characterize this potential relationship.

Methods

Chemicals and reagents. E.Z.N.A.® Genomic DNA Isolation Kits were purchased from Omega Bio-Tek (Norcross, GA). The following deuterated internal standards (IS) were used: d4-DCA (CDN Isotopes; CAS No: 112076-61-6), d4-GCA (CDN Isotopes; CAS No: 1201918-15-1), d4-CDCA (CDN Isotopes; CAS No: 99102-69-9), d4-CA (TRC, Canada; Cat no #: C432603), d4-GCDCA (Iso Sciences, CAS No: 1201918-16-2), lithocholic acid-2,2,4,4-D4 (LCA-D4) (PubChem CID of LCA: 9903, Steralloids). 19 primary BAs were quantified, namely taurine-conjugated cholic acid (T-CA), T-α muricholic acid (T-αMCA), T-β muricholic acid (T-βMCA), T-ω muricholic acid (T-ωMCA), T-chenodeoxycholic acid (T-CDCA), T-ursodeoxycholic acid (T-UDCA), T-hyodeoxycholic acid (T-HDCA), T-deoxycholic acid (T-DCA), T-lithocholic acid (T-LCA), α-muricholic acid (αMCA), β-muricholic acid (βMCA), cholic acid (CA), chenodeoxycholic acid (CDCA), ursodeoxycholic acid (UDCA), ω-muricholic acid (ωMCA), murideoxycholic acid (MDCA), hyodeoxycholic acid (HDCA), deoxycholic acid (DCA), and lithocholic acid (LCA). CA, CDCA, DCA, and LCA were purchased from Sigma Aldrich (St. Louis, Missouri); αMCA, βMCA were purchased from Steraloids (Newport, Rhode Island). ωMCA and T-ωMCA was a kind gift from Dr. Daniel Raftery's laboratory at the University of Washington Northwest Metabolomics Research Center. Other BAs were kindly obtained from the University of Kansas Medical Center. Agilent ZORBAX Eclipse Plus C18 columns were purchased from Waters Corporation (Milford, Massachusetts). The samples were eluted using gradient mobile phases of A (10 mM ammonium acetate in 20% acetonitrile) and B (10 mM ammonium acetate in 80% acetonitrile). The UPLC/MS-MS operating parameters are shown in Supplemental Table 1. All other chemicals and reagents, unless indicated otherwise, were purchased from Sigma-Aldrich (St. Louis, MO).

Animals. FVB/NJ WT male and female mice were purchased from the Jackson Laboratory (aged 21 days upon arrival, n = 5). They were acclimated for at least nine (9) days within the animal facilities before experiments. C57BL/6 WT breeders were purchased from the Jackson Laboratory (Bar Harbor, ME) and then bred in-house (n = 5, both sexes). The knockout mice were all in C57BL/6 background and have been backcrossed at least 10-generations to achieve the homogeneity of the genetic background. Specifically, PXR-null mice were generated and backcrossed into a C57BL/6 background as described previously [51], and pups were obtained from in-house breeders (n = 5 per group). CAR-null mice were generated by Tularik Inc. (South San Francisco, CA) as described previously [52], obtained from University of Kansas Medical Center (Kansas City, KS), and pups were obtained from in-house breeders (n = 5 per group). PXR-CAR-null male and female mice were generated by crossing PXR-null and CAR-null mice (n = 5). Male and female humanized PXR (hPXR) breeders in the FVB/NJ background were a generous gift from Frank Gonzalez (National Cancer Institute, Bethesda, MD) and were bred in-house (n = 5). All mice were individually housed at weaning age in the animal facility at the University of Washington according to the

Association for Assessment and Accreditation of Laboratory Animal Care International guidelines (https://aaalac.org/resources/theguide.cfm). All mice were exposed to laboratory autoclaved rodent diet (LabDiet #5010, LabDiet, St. Louis, MO), non-acidified autoclaved water, and autoclaved Enrich-N'Pure bedding (Andersons, Maumee, OH). All studies were approved by the Institutional Animal Care and Use Committee at the University of Washington. 24-hour fecal samples were collected from mice at adolescent age (1-month of age) and adult age (2-2.5 months of age).

DNA isolation. Total DNA was isolated from frozen fecal samples using E.Z.N.A.® Genomic DNA Isolation Kits (Omega Bio-Tek, Norcross, GA) according to the manufacturer's protocol, and the concentration was quantified using a Qubit fluorometer (Thermo Fisher Scientific, Waltham, MA). The 16S rRNA gene sequencing was performed by Novogene Corporation (Sacramento, CA, 250 bp paired-end, n = 5 per group).

BA quantification. Approximately 50 mg of fecal samples were homogenized in 1 mL of H_2O. 10 µl of IS was added to 200 µl of fecal sample homogenate, mixed, and equilibrated on ice for 5–10 minutes. 1.5 ml of ice-cold alkaline acetonitrile (5% ammonia in acetonitrile) was added to the homogenate, which was then vortexed vigorously and shaken continuously for 1 hour at room temperature. The mixture was then centrifuged at 12,000 *g* for 15 minutes at 4 °C, and the supernatant was collected into 5 mL glass tubes. The pellet was re-suspended in 750 uL of 100% methanol, shaken for 5 minutes, and centrifuged at 15,000 *g* for 20 minutes. The two supernatants obtained were combined, evaporated under vacuum (45 °C) for 4 hours, and reconstituted in 100 µl of 50% methanol. The suspension was transferred into a 0.2 µm Costar Spin-X HPLC microcentrifuge filter (purchased from Corning Inc., Corning, NY), and centrifuged at 12,000 *g* for 10 minutes. 19 BAs were quantified using liquid chromatography-tandem mass spectrometry (LC-MS/MS).

Cytokine quantification. Approximately 20 mg of fecal samples from WT C57BL/6 and WT FVB/NJ mice (adolescent and adult ages, males and females, n = 5 per group) were mixed with PBS (pH = 7.2 supplemented with one (1) mM PMSF [final concentration] and 1X protease inhibitor cocktail [Sigma-Aldrich, catalog number: P8340]) to a final concentration of 100 mg/ml, and were homogenized and centrifuged at 10,000 g at 4 °C for 15 min. The supernatant was collected and diluted 1:1 in the PBS solution described above. The cytokines were quantified using the Mouse Cytokine Array Pro-inflammatory Focused 10-plex (MDF10) (Eve Technologies Corp., Calgary, Alberta) per manufacturer's instructions. The 10 cytokines that were determined include: granulocyte-macrophage colony-stimulating factor (GM-CSF), interferon-gamma (IFNy), interleukin 1 beta (IL-1β), interleukin 2 (IL-2), interleukin 4 (IL-4), interleukin 6 (IL-6), interleukin 10 (IL-10), interleukin 12 (IL-12p70), monocyte chemoattractant protein-1 (MCP-1), and tumor necrosis factor (TNF-α). The ten cytokines were simultaneously quantified in a multiplex panel using a MILLIPLEX Mouse Cytokine/Chemokine 10-plex kit (Millipore, St. Charles, MO, USA) according to the manufacturer's protocol, and was performed using the Luminex™ 100 system (Luminex, Austin, TX, USA). The assay sensitivities of these markers range from 0.4–10.9 pg/mL for the 10-plex. Individual analyte values are available in the MILLIPLEX protocol.

Data analysis. Analysis of FASTQ files was conducted using various python scripts in Quantitative Insights Into Microbial Ecology (QIIME version 1) [53], including de-multiplexing, quality filtering, operational taxonomy unit (OTU) picking, as well as alpha- and beta-diversity determinations. Metagenome functional content was predicted using Phylogenetic Investigation of Communities by Reconstruction of Observed States (PICRUSt) (Langille et al., 2013). Line plots representing the alpha diversity of each group were generated using ggplot2 (v 3.0.0) in R. Three-dimensional Principle Coordinate Analysis (PCoA) plots (beta diversity) were generated using the weighted UniFrac diversity metric in Emperor (Gigascience). OTUs were visualized using stacked bar plots generated in SigmaPlot (Systat Software, Inc). Hierarchical clustering dendrograms (Ward's minimum variance method, distance scale) of the top significantly abundant taxa (abundance > 0.005% $p < 0.05$) were generated using gplots (v 3.0.1) and RColorBrewer (v 1.1-2) in R. Bar plots representing cytokine concentration, BA concentration, and SCFA concentration were generated using ggplot2 (v 3.0.0) in R. Correlation matrices representing SCFA and taxa associations were generated using reshape2 (v 1.4.3) and ggplot2 (v 3.0.0) in R.

Asterisks (*) represent significant differences between C57BL/6 and FVB/NJ mice, WT, and nuclear receptor-gene-null mice ($p < 0.05$), and WT and hPXR-TG mice. Statistically significant differences between WT FVB/NJ and C57BL/6 mice, as well as between WT FVB/NJ and hPXR-TG mice were determined using the Student's *t*-test. Statistically significant differences among WT, PXR-null, CAR-null, and PXR-CAR-null mice (all in C57BL/6 background) were determined using one-way ANOVA followed by Duncan's posthoc test in R using the DescTools package (v 0.99.26) or SPSS (IBM SPSS Statistics).

Experimental Design.

The overall experimental design is shown in Fig. 1. Three experimental settings were designed to model the effect of host PXR/CAR genetics on the gut microbiome. In Study 1, two commonly used laboratory mouse strains with known genetic variations [54], namely the C57BL/6 and FVB/NJ mice, were selected to determine how general differences in host genetics regulate the composition and function of the gut microbiome. It has been reported that FVB mice had a higher hepatic expression of PXR and CAR than C57BL/6 mice [55] (Supplemental Fig. 1). In Study 2, we focused on the necessity of the host PXR and CAR on the basal regulation of gut microbiome, using PXR-null, CAR-null, and PXR-CAR-double null mice (all in C57BL/6 background). In Study 3, we compared the gut microbiomes between the mice that carry mPXR vs. the mice that carry hPXR (both in FVB background), to determine how species-differences of this host drug-receptor modulate the gut microbiome. Due to the markedly reduced pregnancy rate and litter size of the hCAR-TG colony, the comparison of human CAR vs. mCAR was not part of the scope of the present study.

Results

Unveiling the effect of host genetics on gut microbiome using high (FVB) vs. low (C57BL/6) PXR/CAR expressers

Figure 2 shows the alpha diversity (chao1 index), which quantifies the richness of taxa (Fig. 2A), as well as the beta diversity, which quantifies the differences in microbiome among different groups (Fig. 2B), in male and female C57BL/6 and FVB/NJ mice at adolescent and adult ages. FVB/NJ mice had higher microbial richness compared to their C57BL/6 counterparts in both developmental ages and sexes (Fig. 2A). Principle coordinate analysis (PCoA) of the weighted UniFrac measurements showed distinct separations between the microbiomes of FVB/NJ and C57BL/6 mouse strains at both ages and sexes (Fig. 2B).

As shown in Fig. 3A, *Lactococcus*, which may be associated with anti-inflammatory pathways, was specifically colonized in C57BL/6 mice but not in FVB/NJ mice [56]. Conversely, the pro-inflammatory *Acinetobacter* [57, 58], and *E. dolichum*, which is enriched in the Western diet [59], were explicitly colonized in FVB/NJ mice but not in C57BL/6 mice. The most abundant taxa and all differentially regulated taxa in the feces of FVB and C57BL/6 mice are shown in Supplemental Fig. 2 and Supplemental Fig. 3. Interestingly, the abundance of *Paraprevotellaceae Prevotella* sp. was higher in FVB/NJ mice than in C57BL/6 mice at both ages and sexes, except for adolescent females. To note, *Prevotella* has been shown to exhibit increased inflammatory properties as demonstrated by enhanced release of inflammatory mediators from immune cells [60], and the abundance of *Paraprevotellaceae* family has been shown to be higher in IBD [61]. The *Turicibacter* genus was also higher in both FVB/NJ adolescent males and females as compared to their C57BL/6 counterparts, and this pro-inflammatory taxon has been shown to be positively linked to TNFα levels [62].

As shown in Supplemental Fig. 4, to predict the metagenomic functional content of the gut microbiome in FVB/NJ and C57BL/6 mice, Phylogenetic Investigation of Communities by Reconstruction of Unobserved States (PICRUSt) was performed based on the QIIME output. Interestingly, between the two mouse strains, males exhibited higher numbers of predicted functional changes than females at both ages. Pathways enriched were classified into 5 main groups, namely cellular processes, environmental information processing, genetic information processing, metabolism, and organismal systems. Metabolism was the largest category for all groups, with 78 pathways enriched in adolescent males, 104 pathways enriched in adult males, 4 pathways enriched in adolescent females, and 6 enriched in adult females. Overall, the predicted pathways were decreased in C57BL/6 mice and increased in FVB/NJ mice.

The pro-inflammatory microbial signature in FVB mice led us to hypothesize that the basal differences in the gut microbiome of the two mouse strains make FVB/NJ mice more prone to pro-inflammatory signaling under basal conditions. To test this hypothesis, cytokines were quantified from C57BL/6 and FVB/NJ mice to assess how strain differences affect inflammation (Fig. 3B). Overall, pro-inflammatory cytokines were higher in feces of FVB/NJ mice. In particular, MCP-1 had the most significant difference in concentration in all four (4) groups, followed by IL-12, and IL-6. TNFα was higher only in adult female FVB/NJ mice. To note, the anti-inflammatory cytokine IL-10, which is known to increase during inflammation to suppress IL-12 [63], was also higher in FVB/NJ than C57BL/6 mice in males and adult females, indicating a compensatory response.

In summary, profound basal differences in gut microbiome composition were observed between FVB/NJ and C57BL/6 mouse strains. Specifically, we showed that under basal conditions, FVB mice, which had higher basal PXR and CAR expression, have higher richness of the gut microbiome, with a pro-inflammatory microbial signature, corresponding to multiple elevated pro-inflammatory cytokines in feces. This basal configuration may prevent invasions by pathogens through enhanced immune surveillance [64].

Understanding the necessity of host nuclear receptors PXR and CAR on the constitutive regulation of the gut microbiome

16S rRNA gene sequencing was conducted on feces collected over a 24-hour period of adolescent and adult aged WT, PXR-null, CAR-null, and PXR-CAR-double null male and female mice (all in the C57BL/6 background, n = 5 per group), to determine the necessity of host nuclear receptors on the composition and function of the gut microbiome. As shown in Fig. 4A, the alpha diversity of PXR and CAR single or double knockout mice tended to have greater richness than WT controls in all groups, and this trend was especially prominent for PXR-CAR double null mice. The only exception was in adult males; CAR-null mice had the highest richness as compared to the other genotypes. As shown in Fig. 4B, regarding the beta diversity, all four genotypes of mice (WT, PXR-null, CAR-null, and PXR-CAR-double null) exhibited distinct separations among their microbial communities at both ages and sexes. The microbial separations indicate that PXR and CAR are essential and unique modulators of the gut microbiome.

Individual variations contributing to these differences are displayed in the heatmap in Supplemental Fig. 5. In total, 63 taxa were significantly different between WT and PXR-null, CAR-null, and PXR-CAR-null mice (Supplemental Fig. 5). Figure 5 shows the microbial compositional changes at the species level of the top 15 most abundant bacteria as quantified by the percentage of OTUs for the four genotypes of mice (note: the 15th category (Other) includes all other taxa summed together). In all exposure groups, the predominant phyla were *Bacteroidetes*, *Firmicutes*, and *Proteobacteria*. The family *S24-7* was lower in all PXR-null and PXR-CAR-double null groups compared to WT feces, as well as in adult CAR-null males; this taxon has been shown to be decreased during colitis [65]. Bacteria in the family *Helicobacteraceae*, which are positively correlated with IBD [66], increased in relative abundance in PXR-null samples in all groups, as well as both male CAR-null age groups, and CAR-null adult female samples. The pro-inflammatory helicobacter was also higher in the absence of PXR and CAR, whereas the anti-inflammatory *A. muciniphila* was lower in the absence of PXR and CAR (supplemental Fig. 5). *Allobaculum* sp., which is a microbial biomarker that is inversely associated with obesity [67], was higher in all PXR-CAR-null groups, except for adult females. Most notably, as shown in Fig. 6, *Lactobacillus*, which is known to carry bile salt hydrolase (BSH) activity for BA-deconjugation [68, 69], was markedly up-regulated in PXR/CAR-double null mice, and this bacteria also tended to be higher in single receptor gene null mice. *Anaerostipes* sp. decreased in relative abundance in all nuclear receptor-deficient mice of both ages and sexes. This microbe has been shown to have anti-inflammatory effect through producing butyrate [70]. In contrast, the pro-inflammatory *Sutterella* [71], which is enriched in IBD, was up-regulated

in PXR- and CAR-null mice and further up-regulated in the double knockout mice. To note, *Sutterella* is also known to be bile-resistant [72].

The functional predictions of the gut microbiome in the absence of PXR and CAR, as shown in Supplemental Fig. 6, were done using PICRUSt. Females exhibited markedly more functional content predictions than their male counterparts at both developmental ages sampled. In both female ages, absence of PXR caused an increase in the greatest number of pathways, with the opposite being true for CAR-null samples. The PXR-CAR-null group appeared to respond to combinatorial effects of the absence of PXR or CAR, as no change in the abundance of these pathways was seen for these females. The opposite is true for the samples from male mice in that PXR-CAR-null in both ages, and CAR-null in adult males had a marked increase in pathways compared to PXR-null and WT samples. Therefore, sex and host nuclear receptor status affect the function of the gut microbiome in mice.

Because there was a marked increase in the BA-deconjugating *Lactobacillus* in the PXR/CAR-double null mice (and to a lesser extent tended to be higher in the single null mice), we hypothesized that this would result in a reduction in conjugated BAs in feces of the PXR/CAR-null mice. To test this hypothesis, we conducted LC-MS based targeted metabolomics of all major BAs in mice (Fig. 7 and Supplemental Figs. 7–10). As expected, as shown in Fig. 7, the most abundant conjugated BAs in mice, namely T-CA, T-αMCA, T-βMCA, and T-ωMCA, tended to be lower in feces of the PXR/CAR single and double null mice, and the trend was most predominant in the PXR/CAR double null mice. Other minor T-conjugated secondary BAs, such as T-HDCA T-UDCA, were also down-regulated in the knockout mice in an age and sex-dependent manner (Supplemental Figs. 7–10). We also observed an increase in the major unconjugated secondary BA LCA in adolescent PXR/CAR double null mice of both sexes (Supplemental Figs. 7 and 9). However, several other unconjugated secondary BAs were lower in adult PXR/CAR null mice. The inconsistency of the regulatory patterns of the unconjugated secondary BAs patterns in feces may be due to the hydrophobic nature of these BA species, leading to increased body retention and lack of excretion into the fecal compartment. Because unconjugated BAs are more pro-inflammatory than conjugated BAs [9], enhanced BA de-conjugation may prime the host for inflammation related diseases.

Comparison between mouse and human PXR in regulating the gut microbiome

To compare the role of mouse and human PXR genes on the composition and function of the gut microbiome, 16S rRNA gene sequencing was conducted on feces collected over a 24-hour period of adolescent and adult aged wild type (WT) and hPXR-TG male and female mice (n = 5 per group). The overall microbial richness was similar between WT and hPXR-TG mice, except for adolescent males, as evidenced by a higher microbial richness in hPXR-TG mice (Fig. 8A). As shown in Fig. 8B, in all 4 comparisons, hPXR-TG and WT mice exhibited distinct separations between their microbial communities as measured by beta diversity (weighted uniFrac).

In total, 27 taxa with an abundance above 0.00005 were significantly different between WT and hPXR-TG mice (Supplemental Fig. 11). Figure 9 shows the top 15 species level compositional changes of the gut microbiome as quantified by % OTUs. In all groups, the predominant phyla were *Bacteroidetes*, *Firmicutes*,

Tenericutes, and *Verrucomicrobia*, plus *Proteobacteria* in both adult groups and adolescent males. The most predominant difference was a relative increase in *Prevotella* in hPXR-TG mice.

As shown in Supplemental Fig. 12, PICRUSt was used to predict the effect of host nuclear receptor genotype on the metagenomic functional content of the gut microbiome in mice. Adult male hPXR-TG mice were the only group with altered functional pathways. These 21 pathways are: lysine degradation, styrene degradation, aminobenzoate degradation, sulfur metabolism, limonene and pinene degradation, atrazine degradation, biosynthesis of siderophore group nonribosomal peptides, biosynthesis of unsaturated fatty acids, arachidonic acid metabolism, retinol metabolism, chlorocyclohexane and chlorobenzene degradation, bacterial invasion of epithelial cells, proximal tubule bicarbonate reclamation, metabolism of cofactors and vitamins, ion channels, flavonoid biosynthesis, cytochrome P450-mediated xenobiotic metabolism, caprolactam degradation, tryptophan metabolism, and cell motility and secretion. Notably, as a group, all of these pathways decreased in the adult male hPXR-TG mice, with some individual variation. Therefore, species specificity of PXR (i.e. mPXR vs. hPXR) affects the predicted functional differences of the gut microbiome, in a sex- and age-specific manner.

As shown in Fig. 10, BA profiles were different between WT and hPXR-TG mice. Specifically, the largest increase in relative concentration occurred with the secondary BA DCA in hPXR-TG adult male mice, and this trend was seen in the other groups as well. The primary BA CA, which is the precursor of DCA, also tended to be higher in hPXR-TG mice at all 4 comparisons. Conversely, the major secondary BA T-ωMCA tended to be lower in hPXR-TG mice in all 4 comparisons, whereas its unconjugated form ωMCA also tended to be lower in female hPXR-TG mice. Regarding other minor BAs in feces, HDCA was lower in both hPXR-TG adult mice groups, with this trend observed in the adolescent mice, and UDCA was higher in adolescent male and adult female hPXR-TG mice, with this trend continuing in the other groups as well.

Discussion

Through three independent experimental settings, the present study has determined that host genetics, and differences in the xenobiotic-sensing nuclear receptors PXR and CAR in particular, profoundly influence the composition and predicted functions of the gut microbiome, as well as BA metabolism. Specifically, differences in the gut microbiome among individuals with genetic variations may contribute to the basal gut cytokine levels that could predispose certain individuals to GI inflammation. The presence of the drug receptors PXR and CAR prevents the bloom of other types of bacteria that contribute to the richness of the gut microbiome, likely serving a protective mechanism against opportunistic bacteria that may be harmful to the host. The absence of PXR and CAR also led to an increase in the *Lactobacillus* genus, corresponding to reduced taurine-conjugated BAs. Lastly, species differences in PXR (mPXR vs. hPXR) also profoundly altered the gut microbiome, including higher *Prevotella* as well as lower *A. muciniphila*, both of which are hallmarks of inflammatory bowel disease [73, 74], thus caution is warranted when using WT mouse models to study PXR and inflammation, as mPXR carriers may be more resistant to GI inflammation than hPXR carriers.

Just as humans have inter-individual and inter-population genetic differences, strains of mice also differ genetically. Multiple studies have explored the effects of a treatment on the gut microbiota of C57BL/6 and FVB/NJ mice, but to date none have examined the basal regulation of the gut microbiome in these mice. The first part of this study creates a model for how host genetic differences affect the composition and function of the gut microbiome using fecal samples as proxy from the two most widely used laboratory strains of mice.

Higher microbial richness (alpha diversity, Chao1 index) was observed in FVB/NJ mice compared to C57BL/6 mice in both ages and sexes (Fig. 2A), and these strains of mice exhibited distinctly separated communities of microbiota in all groups as well (Fig. 2B). The largest difference in relative abundance of bacteria was the lower abundance of *Prevotellaceae Prevotella* sp. in FVB/NJ mice in all groups (Supplemental Fig. 2). The lower levels of *Prevotellaceae Prevotella* sp. in FVB/NJ mice were accompanied by an increase in multiple other taxa, possibly explaining the differing alpha and beta diversities. These taxa were *Paraprevotellaceae Prevotella* sp., *Anaeroplasma* sp., a member of the *RF32* order, *Acinetobacter* sp., and *E. dolichum*. Multiple taxa were observed in lower abundance in FVB/NJ mice compared to C57BL/6 mice as well, including *Enterococcus* sp., *Lactococcus* sp., and *Carnobacterium* sp. (Supplemental Fig. 3).

The majority of the species changed between the two strains have been associated with inflammation. For example, *Prevotellaceae Prevotella* sp., which decreased in relative abundance in FVB/NJ mice, promotes mucosal inflammation by stimulating the Th17 immune response via epithelial cell production of IL-8, IL-6, and CCL20 [60]. *Prevotellaceae Prevotella* sp. has been further implicated in IBD through its ability to exacerbate DSS-induced colitis via activation of the inflammasome [75]. The genus *Enterococcus*, which also decreased in these mice, has been implicated in infection and increasing susceptibility to IBD [76]. *Carnobacterium* sp., which is found in both extreme temperature and animal environments, potentially contains mucin-degrading abilities [77]. The genus *Lactococcus* is well known for its anti-inflammatory capabilities, has been shown to ameliorate colitis, and also protects the liver from inflammation [56, 78]. Several taxa were also higher in FVB/NJ mice. *Anaeroplasma* sp., which potentially has anti-inflammatory function by inducing the anti-inflammatory cytokine TGF-β, has also been associated with existing in lower relative abundance in hypercholesterolemia subjects leading to an unfavorable lipid profile [79]. The order *RF32* has been correlated with damaged histopathology and colonic inflammation in mice with colitis [80]. *Acinetobacter* sp. has also been correlated with inflammation through the induced signaling of TLR2 and TLR4, which activate the immune response [81]. *E. dolichum* has been shown to produce propionate, which potentially contributes to the inflammatory disease relapsing polychondritis (RP) by continuously stimulating intestinal regulatory T (Treg) cells to produce IL-10, leading to hyporesponsiveness of the Treg cells to mitogen stimulation [82]. In addition to this, *E. dolichum* has been associated with Western diets, and frailty [83–86]. Therefore, the strain differences including differing basal expression levels of PXR and CAR (Supplemental Fig. 1), affect the abundance of inflammation-related bacteria.

Due to the inflammation-related bacterial changes, we decided to measure cytokine levels in these mice (Fig. 3B). Overall, cytokines increased in relative concentration and abundance in FVB/NJ mice. Interestingly, the largest increase was exhibited by MCP-1, which serves to regulate the migration and infiltration of monocytes, memory T lymphocytes, and natural killer (NK) cells to sites of inflammation, both within mice and humans [87]. IL-10, IL-12, and IL-6 increased in relative concentration in FVB/NJ mice as well. The increase in the anti-inflammatory cytokine IL-10 is potentially due to the concomitant increase in IL-12, because IL-10 has been shown to be induced during inflammation to suppress IL-12 [63], indicating a compensatory response. Notably, the cytokines which increased in FVB/NJ mice are affiliated with a type-1 inflammation response. While IL-4 is typically implicated in type-2 inflammation, such as during the pathogenesis of asthma [88], IL-4 also increases during type-1 inflammation [118]. The elevation of the type-1 inflammation response accompanied by the aforementioned bacteria potentially indicates a response to inflammation within the FVB/NJ mice. Whether this type-1 response is caused by LPS from the bacteria or some other mechanism requires further testing. Since this is an animal study, all variation in experimental parameters was restrained to the strains themselves, potentially indicating a genomic difference-mediated effect. FVB/NJ mice contain the G protein-coupled receptor 84 (GPR84) deletion, which leads to accumulation of triglycerides and kidney fibrosis [89]. In fact, GPR84 mRNA expression is elevated during inflammation, and activation of this receptor led to lowered levels of IL-12, IL-6, and MCP-1 in a study by Gagnon et al, indicating a protective response by this receptor [89]. This effect would explain the phenomenon observed in this study.

Regarding the necessity of PXR and CAR on the basal regulation of gut microbiome, observations on microbial compositional and metabolite changes in nuclear receptor gene null mice have provided new insights into the necessity of these host xenobiotic-sensing nuclear receptors on the regulation of gut microbiome under physiological conditions. Especially, the markedly higher proportion of *Lactobacillus* genus in the PXR-CAR-double null mice consistently correspond to a markedly decrease in major T-BAs in feces. Many species and strains of the *Lactobacillus* genus carry BSH that deconjugates the taurine and glycine molecules from BAs [68, 69, 90–95]; in mice, the predominant effect is expected to be T-BA deconjugation, because taurine conjugation is a predominant pathway in mice over glycine conjugation. We have previously demonstrated that pharmacological activation of PXR and CAR leads to decreased gene abundance of the BSH in intestinal content [49]. Findings from the present study further support the inhibitory roles of PXR and CAR in the microbial BSH activities.

Lactobacillus tended to be higher in PXR- and/or CAR-single null mice, although statistical significance was not achieved (Fig. 6), whereas the major T-BAs were significantly lower in single receptor gene null mice. This indicates that other bacteria that remain to be characterized may also contribute to T-BA deconjugation in PXR- and CAR-null mice. Although most abundant T-BAs were lower in the PXR-null, CAR-null, and PXR-CAR-double null mice, the unconjugated BAs did not increase in feces, except for the adolescent females, where there was an apparent increase in unconjugated αMCA, βMCA in all three null mouse genotypes, as well as an increase in CA in PXR-null mice, and these unconjugated BAs are all major primary BAs synthesized from the liver. Conversely, certain unconjugated secondary BAs were lower in the receptor gene null mice, and this pattern was especially prominent in the adult age for all the

three null genotypes. This indicates that the absence of the host PXR and/or CAR receptor may negatively impact the microbial dehydroxylase activities, either through lowering the bacteria that carry the dehydroxylase genes, or through inhibiting the enzyme activities, through altering the intestinal environment through mechanisms that remain to be characterized.

The last part of this study examined the species differences of PXR on the gut microbiome, by comparing humanized-PXR-transgenic (hPXR-TG) mice and WT mice with murine PXR, both within the FVB/NJ background. Even though murine PXR and human PXR share roughly 82% DNA and 77% protein identity, differences in gut microbiome composition were observed between the two mouse genotypes (NCBI HomoloGene).

While higher microbial richness (alpha diversity, Chao1 index) was only observed in adolescent male hPXR-TG mice compared to WT (Fig. 8A), fecal microbial communities were strikingly separated (beta diversity) between the PXR species types in both ages and sexes (Fig. 8B). While *Paraprevotellaceae Prevotella* sp. was responsible for the largest increase in relative abundance in hPXR-TG mice compared to WT, multiple other taxa increased as well, including *AF12* sp. (Fig. 9 & Supplemental Fig. 11). Interestingly, a member of the *Christensenellaceae* family and *Desulfovibrio* sp. increased in relative abundance only in adolescent hPXR-TG mice of both sexes, and *Parabacteroides* sp., a member of the *Bacteroidales* order, and a member of the *YS2* order increased only in adult hPXR-TG mice of both sexes, possibly showing an age-mediated species effect of PXR on gut microbiota. Taxa decreased in hPXR-TG mice as well, most notably including a member of the *RF39* order (class *Mollicutes*) and *A. muciniphila*. An age effect persisted as well in that a member of the *Clostridiales* order and *Anaeroplasma* sp. decreased solely in adolescent hPXR-TG mice (Supplemental Fig. 11).

The large increase in *Paraprevotellaceae Prevotella* sp. in hPXR-TG mice may partially explain the differences in beta diversity observed between the two PXR species differences. Bacteria in this family have been associated with traditional societies' microbiota, with multiple studies finding a correlation between *Paraprevotellaceae* abundance and carbohydrate-heavy diets [15, 96, 97]. Interestingly, male hPXR-TG mice of both ages exhibited an increase in the relative concentration of propionic acid compared to WT mice, which is a conjugated form of the SCFA propionate. A study by Yun et al. found that *Paraprevotellaceae* contributes to propionate formation in a Korean cohort, and this effect is mirrored in another study by Li et al., where an increase in *Paraprevotellaceae* is correlated with an increase in propionate, acetate, and butyrate in silk deer fed oak leaves [98, 99]. Therefore, the observed increase in propionate in male hPXR-TG mice raises the possibility that this is related to the increased relative abundance of *Paraprevotellacea Prevotella* sp.

A member of the *AF12* genus also increased in relative abundance in all groups of hPXR-TG mice. *AF12* sp. is an under-characterized microbe, with some literature finding a correlation between higher abundance and lower body weight, although some evidence is conflicting [100–103]. Additionally, *AF12* sp. has been observed to increase in relative abundance after dietary supplementation of the herbal remedies daikenchuto and the Lingzhi mushroom (*G. lucidum*) [104, 105]. In particular, in Meneses et al.,

the increase in the relative abundance of *AF12* after Lingzhi mushroom consumption by C57BL/6 mice was followed by lowered cholesterol and greater excretion of fecal bile acids [105]. This study observed increased levels of cholic acid (CA) and deoxycholic acid (DCA) in hPXR-TG mice, which may be related to the increase in *AF12* sp. (Fig. 10).

Lastly, *A. muciniphila* decreased in relative abundance in hPXR-TG mice. *A. muciniphila* is a notable bacterial species with mucin-degrading abilities, which has been linked to anti-inflammatory function in liver injury and in diseases such as inflammatory bowel disease (IBD), potentially through its ability to improve an injured gut barrier [106–109]. Therefore, this decrease in *A. muciniphila* may lead to susceptibility for hPXR-TG mice to IBD. Interestingly, hPXR-TG mice are used to study IBD, such as in Dou et al., where hPXR-TG mice were treated with DSS to induce colitis, and then treated with isorhamnetin, a PXR agonist in order to study its effects on ameliorating IBD [110]. The propensity for hPXR-TG mice to already be predisposed to colitis through decreased *A. muciniphila* before DSS treatment throws into question the mechanisms by which PXR agonist IBD treatments work – do they treat the underlying *A. muciniphila* underabundance or the damage caused by DSS; or both? In another study, Cheng et al. treated hPXR-TG mice with rifaximin, a potent PXR agonist used to treat IBD, and found that chronic exposure to rifaximin causes hepatic steatosis, compared to treated WT and treated PXR-null mice [111]. As noted above, hPXR-TG mice are deficient in *A. muciniphila*, potentially increasing their susceptibility to inflammation and liver injury, and so the results in this study may be due to the presence of hPXR rather than rifaximin.

DCA is a bacterially derived secondary bile acid, which has been shown to correlate with colon cancer [112]. DCA increased in hPXR-TG mice, possibly indicating that human PXR increases susceptibility to colon cancer compared to its mouse equivalent. Interestingly, CA was also increased in hPXR-TG mice, possibly indicating that DCA was formed via bacterial deconjugation mechanisms. This proposed mechanism is further confirmed by the observation that the conjugated form of CA, taurocholic acid (TCA), was unchanged, indicating CA and DCA were not increased through *de novo* synthesis in the liver.

This is the first study to characterize the sex- and age-related differences between human and murine PXR on the murine gut microbiome, and the subsequent effects of PXR and CAR expression on immune response and bile acid metabolism.

Conclusions

Well-known as xenobiotic-sensing receptors, pharmacologically activated PXR and CAR have been shown to have anti-inflammatory and cytoprotective effects [113–115], as well as lead to a reduction in the BA-deconjugation enzyme BSH and lower hepatic secondary BAs [49]. The present study has been the first to establish the physiological functions of the host PXR and CAR on the compositions of the gut microbiome as well as the microbial functions related to basal immune surveillance and BA metabolism. Specifically, we showed that under basal conditions, high PXR/CAR expressers have higher richness of the gut microbiome and multiple elevated pro-inflammatory cytokines and a pro-inflammatory microbial

signature; together this basal configuration may prevent invasions by pathogens through enhanced immune surveillance. Interestingly, lack of PXR and CAR individually and synergistically increased the richness of the gut microbiome, also accompanied by a pro-inflammatory microbial signature. This suggests that the presence of PXR/CAR is necessary in preventing the disproportional blooming of certain commensal bacteria, which can become pathogenic if they escape their original niche. Lack of both PXR and CAR also reduced BA-deconjugating bacteria and levels of major taurine-conjugated BAs in feces, suggesting increased hydrophobicity of the internal load of unconjugated BAs and the co-substrate taurine, which may further prime the host for inflammatory response induced by secondary insults. Taken together, the bivalent hormetic functions of PXR and CAR under physiological conditions highlight the novel roles of these host drug receptors in modulating the host immune surveillance and BA metabolism through targeting the gut microbiome.

List Of Abbreviations

PXR, pregnane X receptor; CAR, constitutive androstane receptor; BA, bile acid; hPXR-TG, humanized PXR transgenic; BSH, bile salt hydrolase; T-, taurine conjugated; OH, hydroxylated;

GLP-1, glucagon-like peptide-1; TGR-5, Takeda G-protein-coupled receptor 5; SCFAs, short-chain fatty acids; PBDEs, polybrominated diphenyl ethers; CYP, cytochrome P450; EGF, epidermal growth factor; PCBs, polychlorinated biphenyls; DCA, deoxycholic acid; LCA, lithocholic acid; GF, germ free; CV, conventional; SPF, specific-pathogen-free; IBD, inflammatory bowel disease; NF-kB, nuclear factor kappa-light-chain-enhancer of activated B cells; TLR4, toll-like receptor 4; SNP, single-nucleotide polymorphism; TCPOBOP, 1,4-Bis-[2-(3,5-dichloropyridyloxy)]benzene, 3,3',5,5'-Tetrachloro-1,4-bis(pyridyloxy)benzene; CITCO, 6-(4-Chlorophenyl)imidazo[2,1-b][1, 3]thiazole-5-carbaldehyde O-(3,4-dichlorobenzyl)oxime; WT, wild type; YAP, yes-associated protein; NSAID, non-steroidal anti-inflammatory drug; TNF, tumor necrosis factor; IPA, Indole-3 propionic acid; IS, internal standards; CA, cholic acid; MCA, muricholic acid; CDCA, chenodeoxycholic acid; UDCA, ursodeoxycholic acid; HDCA, hyodeoxycholic acid; DCA, deoxycholic acid; LCA, lithocholic acid; GM-CSF, granulocyte-macrophage colony-stimulating factor; IFNy, interferon-gamma; IL, interleukin; MCP-1, monocyte chemoattractant protein-1; LC-MS/MS, liquid chromatography-tandem mass spectrometry; QIIME, Quantitative Insights Into Microbial Ecology; OTUs, operational taxonomy units; PiCRUSt, Phylogenetic Investigation of Communities by Reconstruction of Observed States; PCoA, Principle Coordinate Analysis.

Declarations

- **Ethics approval and consent to participate**

Not applicable.

- **Consent for publication**

Not applicable.

- **Availability of data and material**

The datasets generated during the current study are available in the Dryad database with the Accession Number https://doi.org/10.5061/dryad.5mkkwh72v.

- **Competing interests**

The authors declare that they have no competing interests.

- **Funding**

Supported by National Institutes of Health (NIH) grant ES025708, ES030197, GM111381, the University of Washington Center for Exposures, Diseases, Genomics, and Environment [P30 ES0007033], and the Murphy Endowment; The Peer Reviewed Medical Research Program – Investigator Initiated Research Award under Award No. W81XWH-17-1-0479; NIH grants (CA 222469); Czech Science Foundation [20-00449S]

- **Authors' contributions**

Participated in research design: Little, Cui

Conducted experiments: Little, Dutta, Li, Matson, Shi, Gu, Sridhar, Cui

Contributed new reagents or analytic tools: Gu, Sridhar, Cui

Performed data analysis: Little, Dutta, Li, Matson, Shi

Wrote or contribute to the writing of the manuscript: Little, Dutta, Li, Matson, Shi, Gu, Sridhar, Cui

- **Acknowledgements**

The authors would like to thank the GNAC technical support for the germ-free mouse experiment, Mr. Brian High and John Yokum from UW DEOHS IT team for providing server access, and the members of Dr. Cui laboratory for their help in tissue collection and revising the manuscript.

References

1. Sender R, Fuchs S, Milo R. Are We Really Vastly Outnumbered? Revisiting the Ratio of Bacterial to Host Cells in Humans. Cell. 2016;164:337–40.
2. Luca F, Kupfer SS, Knights D, Khoruts A, Blekhman R. Functional Genomics of Host-Microbiome Interactions in Humans. Trends Genet. 2018;34:30–40.
3. Cresci GA, Bawden E. Gut Microbiome: What We Do and Don't Know. Nutr Clin Pract. 2015;30:734–46.

4. Seekatz AM, Schnizlein MK, Koenigsknecht MJ, Baker JR, Hasler WL, Bleske BE, Young VB, Sun D: **Spatial and Temporal Analysis of the Stomach and Small-Intestinal Microbiota in Fasted Healthy Humans**. *mSphere* 2019, **4**.
5. Klaassen CD, Cui JY. Review: Mechanisms of How the Intestinal Microbiota Alters the Effects of Drugs and Bile Acids. Drug Metab Dispos. 2015;43:1505–21.
6. Ridlon JM, Kang DJ, Hylemon PB, Bajaj JS. Bile acids and the gut microbiome. Curr Opin Gastroenterol. 2014;30:332–8.
7. Watanabe M, Houten SM, Mataki C, Christoffolete MA, Kim BW, Sato H, Messaddeq N, Harney JW, Ezaki O, Kodama T, et al. Bile acids induce energy expenditure by promoting intracellular thyroid hormone activation. Nature. 2006;439:484–9.
8. Li T, Apte U. Bile Acid Metabolism and Signaling in Cholestasis, Inflammation, and Cancer. Adv Pharmacol. 2015;74:263–302.
9. Allen K, Jaeschke H, Copple BL. Bile acids induce inflammatory genes in hepatocytes: a novel mechanism of inflammation during obstructive cholestasis. Am J Pathol. 2011;178:175–86.
10. Heinken A, Ravcheev DA, Baldini F, Heirendt L, Fleming RMT, Thiele I. Systematic assessment of secondary bile acid metabolism in gut microbes reveals distinct metabolic capabilities in inflammatory bowel disease. Microbiome. 2019;7:75.
11. Hang S, Paik D, Yao L, Kim E, Trinath J, Lu J, Ha S, Nelson BN, Kelly SP, Wu L, et al. Bile acid metabolites control TH17 and Treg cell differentiation. Nature. 2019;576:143–8.
12. Lindenbaum J, Rund DG, Butler VP Jr, Tse-Eng D, Saha JR. Inactivation of digoxin by the gut flora: reversal by antibiotic therapy. N Engl J Med. 1981;305:789–94.
13. Scarpignato C, Dolak W, Lanas A, Matzneller P, Renzulli C, Grimaldi M, Zeitlinger M, Bjarnason I. Rifaximin Reduces the Number and Severity of Intestinal Lesions Associated With Use of Nonsteroidal Anti-Inflammatory Drugs in Humans. Gastroenterology. 2017;152:980–2 e983.
14. Fu ZD, Selwyn FP, Cui JY, Klaassen CD. RNA-Seq Profiling of Intestinal Expression of Xenobiotic Processing Genes in Germ-Free Mice. Drug Metab Dispos. 2017;45:1225–38.
15. Li CY, Lee S, Cade S, Kuo LJ, Schultz IR, Bhatt DK, Prasad B, Bammler TK, Cui JY. Novel Interactions between Gut Microbiome and Host Drug-Processing Genes Modify the Hepatic Metabolism of the Environmental Chemicals Polybrominated Diphenyl Ethers. Drug Metab Dispos. 2017;45:1197–214.
16. Oladimeji PO, Chen T. PXR: More Than Just a Master Xenobiotic Receptor. Mol Pharmacol. 2018;93:119–27.
17. Aleksunes LM, Klaassen CD. Coordinated regulation of hepatic phase I and II drug-metabolizing genes and transporters using AhR-, CAR-, PXR-, PPARalpha-, and Nrf2-null mice. Drug Metab Dispos. 2012;40:1366–79.
18. Banerjee M, Robbins D, Chen T. Targeting xenobiotic receptors PXR and CAR in human diseases. Drug Discov Today. 2015;20:618–28.

19. Mutoh S, Sobhany M, Moore R, Perera L, Pedersen L, Sueyoshi T, Negishi M. Phenobarbital indirectly activates the constitutive active androstane receptor (CAR) by inhibition of epidermal growth factor receptor signaling. Sci Signal. 2013;6:ra31.
20. Watkins RE, Wisely GB, Moore LB, Collins JL, Lambert MH, Williams SP, Willson TM, Kliewer SA, Redinbo MR. The human nuclear xenobiotic receptor PXR: structural determinants of directed promiscuity. Science. 2001;292:2329–33.
21. Ohbuchi M, Yoshinari K, Kaneko H, Matsumoto S, Inoue A, Kawamura A, Usui T, Yamazoe Y. Coordinated roles of pregnane X receptor and constitutive androstane receptor in autoinduction of voriconazole metabolism in mice. Antimicrob Agents Chemother. 2013;57:1332–8.
22. Li CY, Dempsey JL, Wang D, Lee S, Weigel KM, Fei Q, Bhatt DK, Prasad B, Raftery D, Gu H, Cui JY. PBDEs Altered Gut Microbiome and Bile Acid Homeostasis in Male C57BL/6 Mice. Drug Metab Dispos. 2018;46:1226–40.
23. Pencikova K, Svrzkova L, Strapacova S, Neca J, Bartonkova I, Dvorak Z, Hyzdalova M, Pivnicka J, Palkova L, Lehmler HJ, et al. In vitro profiling of toxic effects of prominent environmental lower-chlorinated PCB congeners linked with endocrine disruption and tumor promotion. Environ Pollut. 2018;237:473–86.
24. Zhou H, Hylemon PB. Bile acids are nutrient signaling hormones. Steroids. 2014;86:62–8.
25. Xu C, Huang M, Bi H. PXR- and CAR-mediated herbal effect on human diseases. Biochim Biophys Acta. 2016;1859:1121–9.
26. Bhutia YD, Ogura J, Sivaprakasam S, Ganapathy V. Gut Microbiome and Colon Cancer: Role of Bacterial Metabolites and Their Molecular Targets in the Host. Curr Colorectal Cancer Rep. 2017;13:111–8.
27. Sivaprakasam S, Bhutia YD, Ramachandran S, Ganapathy V. **Cell-Surface and Nuclear Receptors in the Colon as Targets for Bacterial Metabolites and Its Relevance to Colon Health**. *Nutrients* 2017, 9.
28. Selwyn FP, Cheng SL, Bammler TK, Prasad B, Vrana M, Klaassen C, Cui JY. Developmental Regulation of Drug-Processing Genes in Livers of Germ-Free Mice. Toxicol Sci. 2015;147:84–103.
29. Toda T, Saito N, Ikarashi N, Ito K, Yamamoto M, Ishige A, Watanabe K, Sugiyama K. Intestinal flora induces the expression of Cyp3a in the mouse liver. Xenobiotica. 2009;39:323–34.
30. Shah YM, Ma X, Morimura K, Kim I, Gonzalez FJ. Pregnane X receptor activation ameliorates DSS-induced inflammatory bowel disease via inhibition of NF-kappaB target gene expression. Am J Physiol Gastrointest Liver Physiol. 2007;292:G1114–22.
31. Qiu Z, Cervantes JL, Cicek BB, Mukherjee S, Venkatesh M, Maher LA, Salazar JC, Mani S, Khanna KM. Pregnane X Receptor Regulates Pathogen-Induced Inflammation and Host Defense against an Intracellular Bacterial Infection through Toll-like Receptor 4. Sci Rep. 2016;6:31936.
32. Ranhotra HS, Flannigan KL, Brave M, Mukherjee S, Lukin DJ, Hirota SA, Mani S. **Xenobiotic Receptor-Mediated Regulation of Intestinal Barrier Function and Innate Immunity**. *Nucl Receptor Res* 2016, 3.
33. Huang K, Mukherjee S, DesMarais V, Albanese JM, Rafti E, Draghi Ii A, Maher LA, Khanna KM, Mani S, Matson AP. Targeting the PXR-TLR4 signaling pathway to reduce intestinal inflammation in an

experimental model of necrotizing enterocolitis. Pediatr Res. 2018;83:1031–40.

34. Venkatesh M, Mukherjee S, Wang H, Li H, Sun K, Benechet AP, Qiu Z, Maher L, Redinbo MR, Phillips RS, et al. Symbiotic bacterial metabolites regulate gastrointestinal barrier function via the xenobiotic sensor PXR and Toll-like receptor 4. Immunity. 2014;41:296–310.
35. Ma N, Guo P, Zhang J, He T, Kim SW, Zhang G, Ma X. Nutrients Mediate Intestinal Bacteria-Mucosal Immune Crosstalk. Front Immunol. 2018;9:5.
36. He J, Gao J, Xu M, Ren S, Stefanovic-Racic M, O'Doherty RM, Xie W. PXR ablation alleviates diet-induced and genetic obesity and insulin resistance in mice. Diabetes. 2013;62:1876–87.
37. Gao J, He J, Zhai Y, Wada T, Xie W. The constitutive androstane receptor is an anti-obesity nuclear receptor that improves insulin sensitivity. J Biol Chem. 2009;284:25984–92.
38. Ihunnah CA, Jiang M, Xie W. Nuclear receptor PXR, transcriptional circuits and metabolic relevance. Biochim Biophys Acta. 2011;1812:956–63.
39. Wang Y, Xiang X, Huang WW, Sandford AJ, Wu SQ, Zhang MM, Wang MG, Chen G, He JQ. Association of PXR and CAR Polymorphisms and Antituberculosis Drug-Induced Hepatotoxicity. Sci Rep. 2019;9:2217.
40. Kublbeck J, Zancanella V, Prantner V, Molnar F, Squires EJ, Dacasto M, Honkakoski P, Giantin M. Characterization of ligand-dependent activation of bovine and pig constitutive androstane (CAR) and pregnane X receptors (PXR) with interspecies comparisons. Xenobiotica. 2016;46:200–10.
41. LeCluyse EL. Pregnane X receptor: molecular basis for species differences in CYP3A induction by xenobiotics. Chem Biol Interact. 2001;134:283–9.
42. de Boussac H, Gondeau C, Briolotti P, Duret C, Treindl F, Romer M, Fabre JM, Herrero A, Ramos J, Maurel P, et al. Epidermal Growth Factor Represses Constitutive Androstane Receptor Expression in Primary Human Hepatocytes and Favors Regulation by Pregnane X Receptor. Drug Metab Dispos. 2018;46:223–36.
43. Zhang YK, Lu H, Klaassen CD. Expression of human CAR splicing variants in BAC-transgenic mice. Toxicol Sci. 2013;132:142–50.
44. Park S, Cheng SL, Cui JY. Characterizing drug-metabolizing enzymes and transporters that are bona fide CAR-target genes in mouse intestine. Acta Pharm Sin B. 2016;6:475–91.
45. Elcombe CR, Peffer RC, Wolf DC, Bailey J, Bars R, Bell D, Cattley RC, Ferguson SS, Geter D, Goetz A, et al. Mode of action and human relevance analysis for nuclear receptor-mediated liver toxicity: A case study with phenobarbital as a model constitutive androstane receptor (CAR) activator. Crit Rev Toxicol. 2014;44:64–82.
46. Jiang Y, Feng D, Ma X, Fan S, Gao Y, Fu K, Wang Y, Sun J, Yao X, Liu C, et al. Pregnane X Receptor Regulates Liver Size and Liver Cell Fate by Yes-Associated Protein Activation in Mice. Hepatology. 2019;69:343–58.
47. Whitfield-Cargile CM, Cohen ND, Chapkin RS, Weeks BR, Davidson LA, Goldsby JS, Hunt CL, Steinmeyer SH, Menon R, Suchodolski JS, et al. The microbiota-derived metabolite indole decreases

mucosal inflammation and injury in a murine model of NSAID enteropathy. Gut Microbes. 2016;7:246–61.

48. Caparros-Martin JA, Lareu RR, Ramsay JP, Peplies J, Reen FJ, Headlam HA, Ward NC, Croft KD, Newsholme P, Hughes JD, O'Gara F. Statin therapy causes gut dysbiosis in mice through a PXR-dependent mechanism. Microbiome. 2017;5:95.
49. Dempsey JL, Wang D, Siginir G, Fei Q, Raftery D, Gu H, Yue Cui J. Pharmacological Activation of PXR and CAR Downregulates Distinct Bile Acid-Metabolizing Intestinal Bacteria and Alters Bile Acid Homeostasis. Toxicol Sci. 2019;168:40–60.
50. Cheng SL, Li X, Lehmler HJ, Phillips B, Shen D, Cui JY. Gut Microbiota Modulates Interactions Between Polychlorinated Biphenyls and Bile Acid Homeostasis. Toxicol Sci. 2018;166:269–87.
51. Staudinger JL, Goodwin B, Jones SA, Hawkins-Brown D, MacKenzie KI, LaTour A, Liu Y, Klaassen CD, Brown KK, Reinhard J, et al. The nuclear receptor PXR is a lithocholic acid sensor that protects against liver toxicity. Proc Natl Acad Sci U S A. 2001;98:3369–74.
52. Ueda A, Hamadeh HK, Webb HK, Yamamoto Y, Sueyoshi T, Afshari CA, Lehmann JM, Negishi M. Diverse roles of the nuclear orphan receptor CAR in regulating hepatic genes in response to phenobarbital. Mol Pharmacol. 2002;61:1–6.
53. Caporaso JG, Kuczynski J, Stombaugh J, Bittinger K, Bushman FD, Costello EK, Fierer N, Pena AG, Goodrich JK, Gordon JI, et al. QIIME allows analysis of high-throughput community sequencing data. Nat Methods. 2010;7:335–6.
54. Wong K, Bumpstead S, Van Der Weyden L, Reinholdt LG, Wilming LG, Adams DJ, Keane TM. Sequencing and characterization of the FVB/NJ mouse genome. Genome Biol. 2012;13:R72.
55. Bradford BU, Lock EF, Kosyk O, Kim S, Uehara T, Harbourt D, DeSimone M, Threadgill DW, Tryndyak V, Pogribny IP, et al. Interstrain differences in the liver effects of trichloroethylene in a multistrain panel of inbred mice. Toxicol Sci. 2011;120:206–17.
56. Luerce TD, Gomes-Santos AC, Rocha CS, Moreira TG, Cruz DN, Lemos L, Sousa AL, Pereira VB, de Azevedo M, Moraes K, et al. Anti-inflammatory effects of Lactococcus lactis NCDO 2118 during the remission period of chemically induced colitis. Gut Pathog. 2014;6:33.
57. Jun SH, Lee JH, Kim BR, Kim SI, Park TI, Lee JC, Lee YC. Acinetobacter baumannii outer membrane vesicles elicit a potent innate immune response via membrane proteins. PLoS One. 2013;8:e71751.
58. Kikuchi-Ueda T, Kamoshida G, Ubagai T, Nakano R, Nakano A, Akuta T, Hikosaka K, Tansho-Nagakawa S, Kikuchi H, Ono Y. The TNF-alpha of mast cells induces pro-inflammatory responses during infection with Acinetobacter baumannii. Immunobiology. 2017;222:1025–34.
59. Turnbaugh PJ, Ridaura VK, Faith JJ, Rey FE, Knight R, Gordon JI. The effect of diet on the human gut microbiome: a metagenomic analysis in humanized gnotobiotic mice. Sci Transl Med. 2009;1:6ra14.
60. Larsen JM. The immune response to Prevotella bacteria in chronic inflammatory disease. Immunology. 2017;151:363–74.
61. Omori M, Maeda S, Igarashi H, Ohno K, Sakai K, Yonezawa T, Horigome A, Odamaki T, Matsuki N. Fecal microbiome in dogs with inflammatory bowel disease and intestinal lymphoma. J Vet Med Sci.

2017;79:1840–7.

62. Jones-Hall YL, Kozik A, Nakatsu C. Ablation of tumor necrosis factor is associated with decreased inflammation and alterations of the microbiota in a mouse model of inflammatory bowel disease. PLoS One. 2015;10:e0119441.
63. Rahim SS, Khan N, Boddupalli CS, Hasnain SE, Mukhopadhyay S. Interleukin-10 (IL-10) mediated suppression of IL-12 production in RAW 264.7 cells also involves c-rel transcription factor. Immunology. 2005;114:313–21.
64. Shi N, Li N, Duan X, Niu H. Interaction between the gut microbiome and mucosal immune system. Mil Med Res. 2017;4:14.
65. Osaka T, Moriyama E, Arai S, Date Y, Yagi J, Kikuchi J, Tsuneda S. **Meta-Analysis of Fecal Microbiota and Metabolites in Experimental Colitic Mice during the Inflammatory and Healing Phases**. *Nutrients* 2017, 9.
66. Zhang L, Day A, McKenzie G, Mitchell H. Nongastric Helicobacter species detected in the intestinal tract of children. J Clin Microbiol. 2006;44:2276–9.
67. Ravussin Y, Koren O, Spor A, LeDuc C, Gutman R, Stombaugh J, Knight R, Ley RE, Leibel RL. Responses of gut microbiota to diet composition and weight loss in lean and obese mice. Obesity (Silver Spring). 2012;20:738–47.
68. O'Flaherty S, Briner Crawley A, Theriot CM, Barrangou R: **The Lactobacillus Bile Salt Hydrolase Repertoire Reveals Niche-Specific Adaptation**. *mSphere* 2018, **3**.
69. Ridlon JM, Kang DJ, Hylemon PB. Bile salt biotransformations by human intestinal bacteria. J Lipid Res. 2006;47:241–59.
70. Kant R, Rasinkangas P, Satokari R, Pietila TE, Palva A. **Genome Sequence of the Butyrate-Producing Anaerobic Bacterium Anaerostipes hadrus PEL 85**. *Genome Announc* 2015, 3.
71. Hiippala K, Kainulainen V, Kalliomaki M, Arkkila P, Satokari R. Mucosal Prevalence and Interactions with the Epithelium Indicate Commensalism of Sutterella spp. Front Microbiol. 2016;7:1706.
72. Williams BL, Hornig M, Parekh T, Lipkin WI. **Application of novel PCR-based methods for detection, quantitation, and phylogenetic characterization of Sutterella species in intestinal biopsy samples from children with autism and gastrointestinal disturbances**. *MBio* 2012, 3.
73. Png CW, Linden SK, Gilshenan KS, Zoetendal EG, McSweeney CS, Sly LI, McGuckin MA, Florin TH. Mucolytic bacteria with increased prevalence in IBD mucosa augment in vitro utilization of mucin by other bacteria. Am J Gastroenterol. 2010;105:2420–8.
74. Olbjorn C, Cvancarova Smastuen M, Thiis-Evensen E, Nakstad B, Vatn MH, Jahnsen J, Ricanek P, Vatn S, Moen AEF, Tannaes TM, et al. Fecal microbiota profiles in treatment-naive pediatric inflammatory bowel disease - associations with disease phenotype, treatment, and outcome. Clin Exp Gastroenterol. 2019;12:37–49.
75. Elinav E, Strowig T, Kau AL, Henao-Mejia J, Thaiss CA, Booth CJ, Peaper DR, Bertin J, Eisenbarth SC, Gordon JI, Flavell RA. NLRP6 inflammasome regulates colonic microbial ecology and risk for colitis. Cell. 2011;145:745–57.

76. Golinska E, Tomusiak A, Gosiewski T, Wiecek G, Machul A, Mikolajczyk D, Bulanda M, Heczko PB, Strus M. Virulence factors of Enterococcus strains isolated from patients with inflammatory bowel disease. World J Gastroenterol. 2013;19:3562–72.
77. Iskandar CF, Borges F, Taminiau B, Daube G, Zagorec M, Remenant B, Leisner JJ, Hansen MA, Sorensen SJ, Mangavel C, et al. Comparative Genomic Analysis Reveals Ecological Differentiation in the Genus Carnobacterium. Front Microbiol. 2017;8:357.
78. Jena PK, Sheng L, Liu HX, Kalanetra KM, Mirsoian A, Murphy WJ, French SW, Krishnan VV, Mills DA, Wan YY. Western Diet-Induced Dysbiosis in Farnesoid X Receptor Knockout Mice Causes Persistent Hepatic Inflammation after Antibiotic Treatment. Am J Pathol. 2017;187:1800–13.
79. Granado-Serrano AB, Martin-Gari M, Sanchez V, Riart Solans M, Berdun R, Ludwig IA, Rubio L, Vilaprinyo E, Portero-Otin M, Serrano JCE. Faecal bacterial and short-chain fatty acids signature in hypercholesterolemia. Sci Rep. 2019;9:1772.
80. Castro-Mejia J, Jakesevic M, Krych L, Nielsen DS, Hansen LH, Sondergaard BC, Kvist PH, Hansen AK, Holm TL. Treatment with a Monoclonal Anti-IL-12p40 Antibody Induces Substantial Gut Microbiota Changes in an Experimental Colitis Model. Gastroenterol Res Pract. 2016;2016:4953120.
81. Erridge C, Moncayo-Nieto OL, Morgan R, Young M, Poxton IR. Acinetobacter baumannii lipopolysaccharides are potent stimulators of human monocyte activation via Toll-like receptor 4 signalling. J Med Microbiol. 2007;56:165–71.
82. Shimizu J, Kubota T, Takada E, Takai K, Fujiwara N, Arimitsu N, Murayama MA, Ueda Y, Wakisaka S, Suzuki T, Suzuki N. Propionate-producing bacteria in the intestine may associate with skewed responses of IL10-producing regulatory T cells in patients with relapsing polychondritis. PLoS One. 2018;13:e0203657.
83. Brown K, DeCoffe D, Molcan E, Gibson DL. Diet-induced dysbiosis of the intestinal microbiota and the effects on immunity and disease. Nutrients. 2012;4:1095–119.
84. Pallister T, Jackson MA, Martin TC, Glastonbury CA, Jennings A, Beaumont M, Mohney RP, Small KS, MacGregor A, Steves CJ, et al. Untangling the relationship between diet and visceral fat mass through blood metabolomics and gut microbiome profiling. Int J Obes (Lond). 2017;41:1106–13.
85. Turnbaugh PJ, Backhed F, Fulton L, Gordon JI. Diet-induced obesity is linked to marked but reversible alterations in the mouse distal gut microbiome. Cell Host Microbe. 2008;3:213–23.
86. Jackson MA, Jeffery IB, Beaumont M, Bell JT, Clark AG, Ley RE, O'Toole PW, Spector TD, Steves CJ. Signatures of early frailty in the gut microbiota. Genome Med. 2016;8:8.
87. Deshmane SL, Kremlev S, Amini S, Sawaya BE. Monocyte chemoattractant protein-1 (MCP-1): an overview. J Interferon Cytokine Res. 2009;29:313–26.
88. Dunican EM, Fahy JV. The Role of Type 2 Inflammation in the Pathogenesis of Asthma Exacerbations. Ann Am Thorac Soc. 2015;12(Suppl 2):144–9.
89. Gagnon L, Leduc M, Thibodeau JF, Zhang MZ, Grouix B, Sarra-Bournet F, Gagnon W, Hince K, Tremblay M, Geerts L, et al. A Newly Discovered Antifibrotic Pathway Regulated by Two Fatty Acid Receptors: GPR40 and GPR84. Am J Pathol. 2018;188:1132–48.

90. Chae JP, Valeriano VD, Kim GB, Kang DK. Molecular cloning, characterization and comparison of bile salt hydrolases from Lactobacillus johnsonii PF01. J Appl Microbiol. 2013;114:121–33.
91. De Smet I, Van Hoorde L, Vande Woestyne M, Christiaens H, Verstraete W. Significance of bile salt hydrolytic activities of lactobacilli. J Appl Bacteriol. 1995;79:292–301.
92. Kumar RS, Brannigan JA, Prabhune AA, Pundle AV, Dodson GG, Dodson EJ, Suresh CG. Structural and functional analysis of a conjugated bile salt hydrolase from Bifidobacterium longum reveals an evolutionary relationship with penicillin V acylase. J Biol Chem. 2006;281:32516–25.
93. Foley MH, O'Flaherty S, Barrangou R, Theriot CM. Bile salt hydrolases: Gatekeepers of bile acid metabolism and host-microbiome crosstalk in the gastrointestinal tract. PLoS Pathog. 2019;15:e1007581.
94. Allain T, Chaouch S, Thomas M, Travers MA, Valle I, Langella P, Grellier P, Polack B, Florent I, Bermudez-Humaran LG: **Bile Salt Hydrolase Activities**: **A Novel Target to Screen Anti-Giardia Lactobacilli?** *Front Microbiol* 2018, **9**:89.
95. Allain T, Chaouch S, Thomas M, Vallee I, Buret AG, Langella P, Grellier P, Polack B, Bermudez-Humaran LG, Florent I. Bile-Salt-Hydrolases from the Probiotic Strain Lactobacillus johnsonii La1 Mediate Anti-giardial Activity in Vitro and in Vivo. Front Microbiol. 2017;8:2707.
96. Acharya A, Chan Y, Kheur S, Kheur M, Gopalakrishnan D, Watt RM, Mattheos N. Salivary microbiome of an urban Indian cohort and patterns linked to subclinical inflammation. Oral Dis. 2017;23:926–40.
97. Wu GD, Chen J, Hoffmann C, Bittinger K, Chen YY, Keilbaugh SA, Bewtra M, Knights D, Walters WA, Knight R, et al. Linking long-term dietary patterns with gut microbial enterotypes. Science. 2011;334:105–8.
98. Yun Y, Kim HN, Kim SE, Heo SG, Chang Y, Ryu S, Shin H, Kim HL. Comparative analysis of gut microbiota associated with body mass index in a large Korean cohort. BMC Microbiol. 2017;17:151.
99. Li Z, Wright AD, Liu H, Bao K, Zhang T, Wang K, Cui X, Yang F, Zhang Z, Li G. Bacterial community composition and fermentation patterns in the rumen of sika deer (Cervus nippon) fed three different diets. Microb Ecol. 2015;69:307–18.
100. Lai ZL, Tseng CH, Ho HJ, Cheung CKY, Lin JY, Chen YJ, Cheng FC, Hsu YC, Lin JT, El-Omar EM, Wu CY. Fecal microbiota transplantation confers beneficial metabolic effects of diet and exercise on diet-induced obese mice. Sci Rep. 2018;8:15625.
101. Garcia-Mazcorro JF, Mills D, Noratto G. **Molecular exploration of fecal microbiome in quinoa-supplemented obese mice**. *FEMS Microbiol Ecol* 2016, 92.
102. Chen M, Liao Z, Lu B, Wang M, Lin L, Zhang S, Li Y, Liu D, Liao Q, Xie Z. Huang-Lian-Jie-Du-Decoction Ameliorates Hyperglycemia and Insulin Resistant in Association With Gut Microbiota Modulation. Front Microbiol. 2018;9:2380.
103. Alteber Z, Sharbi-Yunger A, Pevsner-Fischer M, Blat D, Roitman L, Tzehoval E, Elinav E, Eisenbach L. The anti-inflammatory IFITM genes ameliorate colitis and partially protect from tumorigenesis by changing immunity and microbiota. Immunol Cell Biol. 2018;96:284–97.

104. Miyoshi J, Nobutani K, Musch MW, Ringus DL, Hubert NA, Yamamoto M, Kase Y, Nishiyama M, Chang EB. Time-, Sex-, and Dose-Dependent Alterations of the Gut Microbiota by Consumption of Dietary Daikenchuto (TU-100). Evid Based Complement Alternat Med. 2018;2018:7415975.
105. Meneses ME, Martinez-Carrera D, Torres N, Sanchez-Tapia M, Aguilar-Lopez M, Morales P, Sobal M, Bernabe T, Escudero H, Granados-Portillo O, Tovar AR. Hypocholesterolemic Properties and Prebiotic Effects of Mexican Ganoderma lucidum in C57BL/6 Mice. PLoS One. 2016;11:e0159631.
106. Ring C, Klopfleisch R, Dahlke K, Basic M, Bleich A, Blaut M. Akkermansia muciniphila strain ATCC BAA-835 does not promote short-term intestinal inflammation in gnotobiotic interleukin-10-deficient mice. Gut Microbes. 2019;10:188–203.
107. Wu W, Lv L, Shi D, Ye J, Fang D, Guo F, Li Y, He X, Li L. Protective Effect of Akkermansia muciniphila against Immune-Mediated Liver Injury in a Mouse Model. Front Microbiol. 2017;8:1804.
108. Zhao S, Liu W, Wang J, Shi J, Sun Y, Wang W, Ning G, Liu R, Hong J. Akkermansia muciniphila improves metabolic profiles by reducing inflammation in chow diet-fed mice. J Mol Endocrinol. 2017;58:1–14.
109. Reunanen J, Kainulainen V, Huuskonen L, Ottman N, Belzer C, Huhtinen H, de Vos WM, Satokari R. Akkermansia muciniphila Adheres to Enterocytes and Strengthens the Integrity of the Epithelial Cell Layer. Appl Environ Microbiol. 2015;81:3655–62.
110. Dou W, Zhang J, Li H, Kortagere S, Sun K, Ding L, Ren G, Wang Z, Mani S. Plant flavonol isorhamnetin attenuates chemically induced inflammatory bowel disease via a PXR-dependent pathway. J Nutr Biochem. 2014;25:923–33.
111. Cheng J, Krausz KW, Tanaka N, Gonzalez FJ. Chronic exposure to rifaximin causes hepatic steatosis in pregnane X receptor-humanized mice. Toxicol Sci. 2012;129:456–68.
112. Ajouz H, Mukherji D, Shamseddine A. Secondary bile acids: an underrecognized cause of colon cancer. World J Surg Oncol. 2014;12:164.
113. Baskin-Bey ES, Anan A, Isomoto H, Bronk SF, Gores GJ. Constitutive androstane receptor agonist, TCPOBOP, attenuates steatohepatitis in the methionine choline-deficient diet-fed mouse. World J Gastroenterol. 2007;13:5635–41.
114. Baskin-Bey ES, Huang W, Ishimura N, Isomoto H, Bronk SF, Braley K, Craig RW, Moore DD, Gores GJ. Constitutive androstane receptor (CAR) ligand, TCPOBOP, attenuates Fas-induced murine liver injury by altering Bcl-2 proteins. Hepatology. 2006;44:252–62.
115. Cheng J, Shah YM, Gonzalez FJ. Pregnane X receptor as a target for treatment of inflammatory bowel disorders. Trends Pharmacol Sci. 2012;33:323–30.
116. Hogle BC, Guan X, Folan MM, Xie W. PXR as a mediator of herb-drug interaction. J Food Drug Anal. 2018;26:26–31.
117. Chang TK. Activation of pregnane X receptor (PXR) and constitutive androstane receptor (CAR) by herbal medicines. AAPS J. 2009;11:590–601.
118. Matson AP, Zhu L, Lingenheld EG, Schramm CM, Clark RB, Selander DM, Thrall RS, Breen E, Puddington L. Maternal transmission of resistance to development of allergic airway disease. J

Immunol. 2007;179:1282–91.

Figures

Figure 1

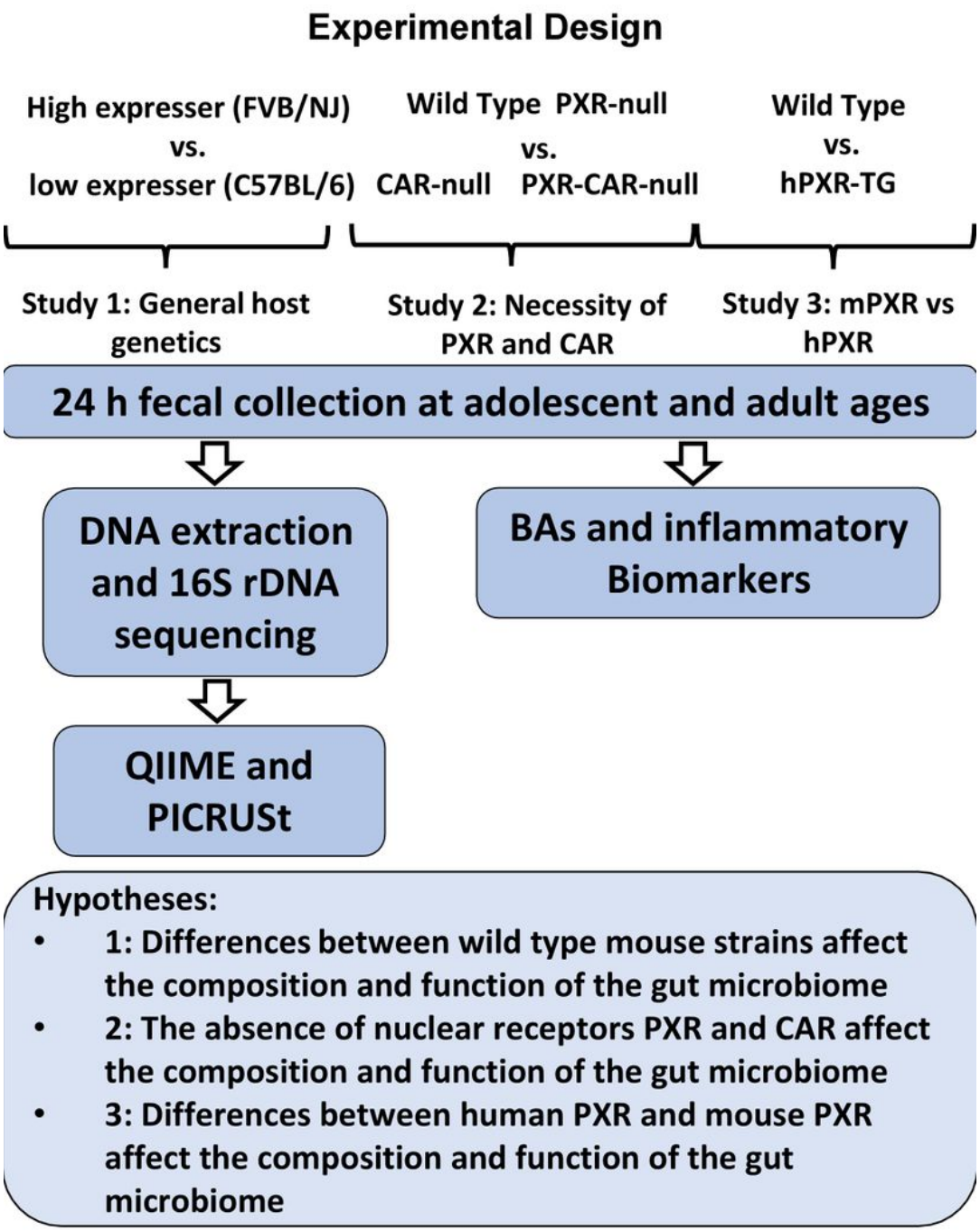

Figure 1

Diagram of the experimental design of this study. To compare the role of differences of two mouse strains that have different PXR/CAR basal levels (Supplemental Figure 1) on the composition and function of the gut microbiome, fecal samples were collected from WT C57BL/6 (low expressers) and WT FVB/NJ (high expressers) male and female mice of adolescent and adult ages (n=5 of each group). To determine the necessity of host nuclear receptors on the composition and function of the gut microbiome, fecal samples were collected from WT, PXR-null, CAR-null, and PXR-CAR-null male and female mice of adolescent and adult ages (n=5 of each group). To compare the role of mouse and human PXR genes on the composition and function of the gut microbiome, fecal samples were collected from WT and hPXR-TG male and female mice of adolescent and adult ages (n=5 of each group). Fecal samples were collected after 24 hours, and 16S rRNA gene sequencing was conducted by amplifying the hypervariable V4 region. Analysis of FASTQ files was conducted using various python scripts in Quantitative Insights Into Microbial Ecology (QIIME) [53], including de-multiplexing, quality filtering, operational taxonomy unit (OTU) picking, as well as alpha- and beta-diversity determinations. Metagenome functional content was predicted using Phylogenetic Investigation of Communities by Reconstruction of Observed States (PICRUSt) (Langille et al., 2013). BAs were quantified using liquid chromatography–tandem mass spectrometry (LC-MS/MS). Cytokines were quantified using the Mouse Cytokine Array Pro-inflammatory Focused 10-plex (MDF10) (Eve Technologies Corp., Calgary, Alberta).

Figure 2

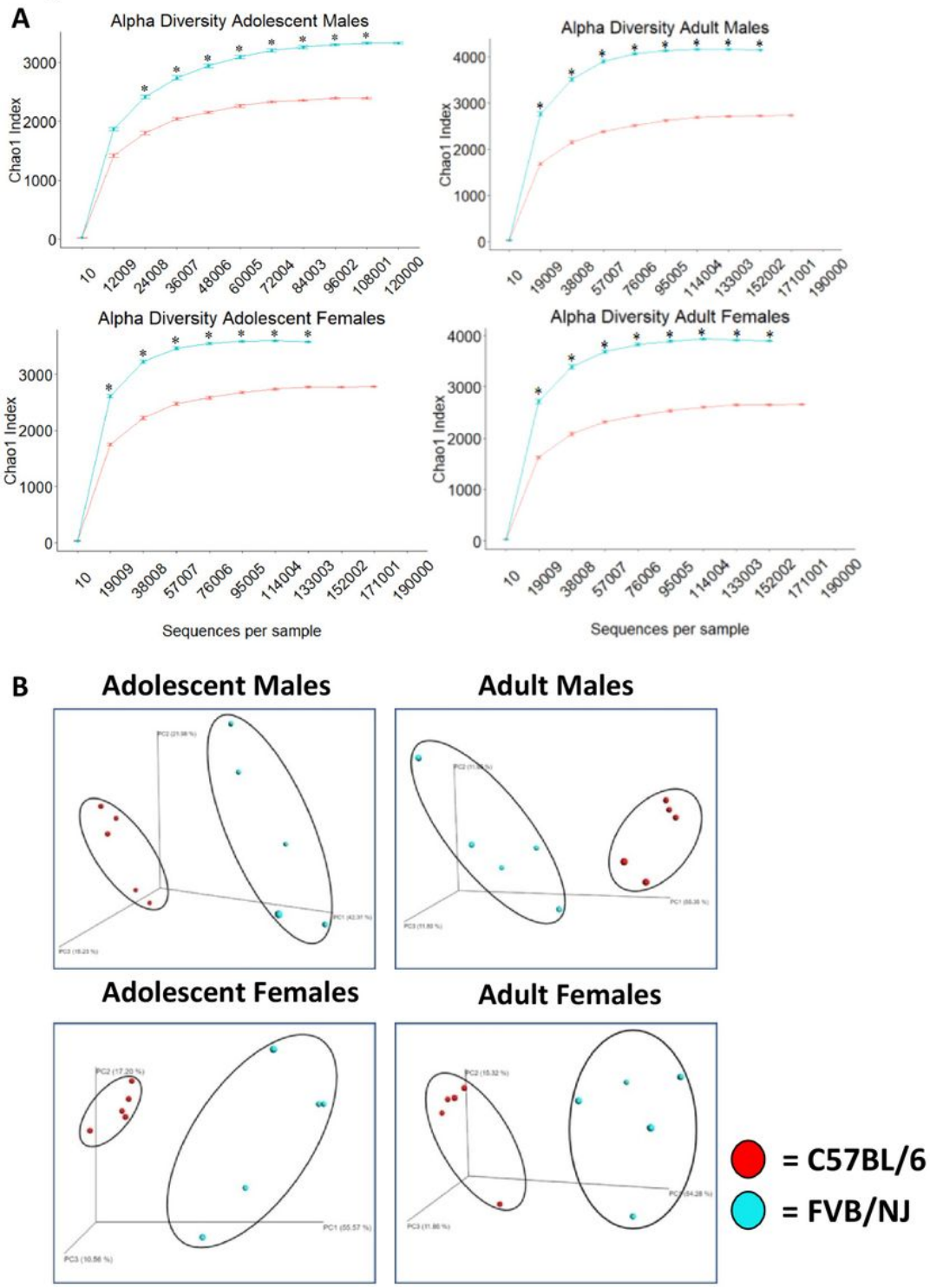

Figure 2

Alpha and beta diversities of C57BL/6 and FVB/NJ mice. A. Alpha diversity of gut microbiota within the low PXR/CAR expressers (C57BL/6) and high PXR/CAR expressers (FVB/NJ mice). Line plots were generated using the R package ggplot. Asterisks represent statistically significant differences compared to C57BL/6 mice (t-test, $P < 0.05$). B. Principal coordinate analysis (PCoA) plots showing the beta

diversities of adolescent male, adult male, adolescent female, and adult female C57BL/6 and FVB/NJ mice.

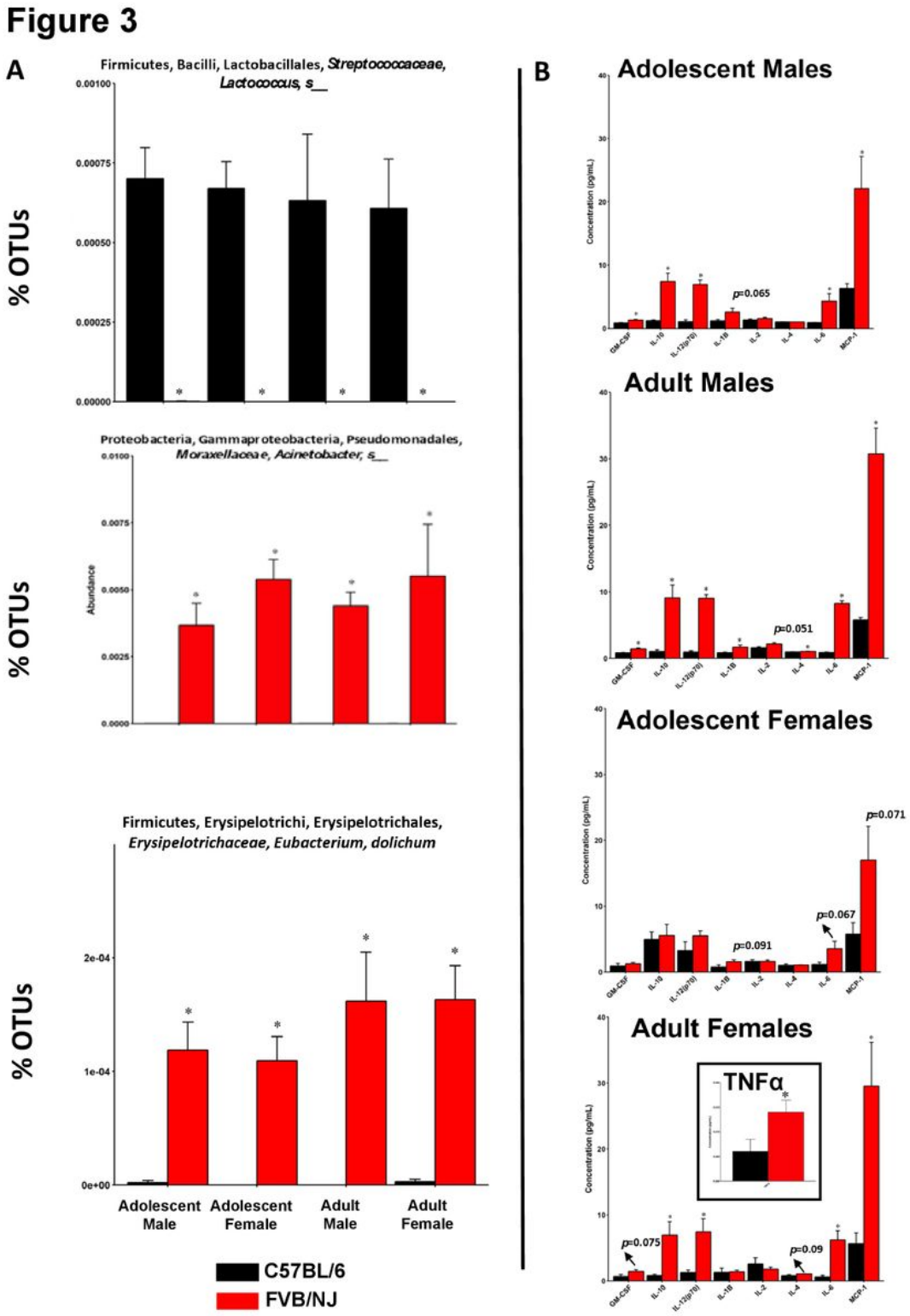

Figure 3

Percentage OTUs of Lactococcus sp., Acinetobacter sp., and E. dolichum, and cytokine concentrations in C57BL/6 and FVB/NJ mice. A. Individual bar plots of Lactococcus sp., Acinetobacter sp., and E. dolichum, are generated by the R package ggplot2. Asterisks represent statistically significant differences

compared to C57BL/6 mice (t-test, $p < 0.05$). B. Bar plots of cytokine concentrations (pg/mL) are generated by the R package ggplot2. Asterisks represent statistically significant differences compared to C57BL/6 mice (t-test, $p < 0.05$).

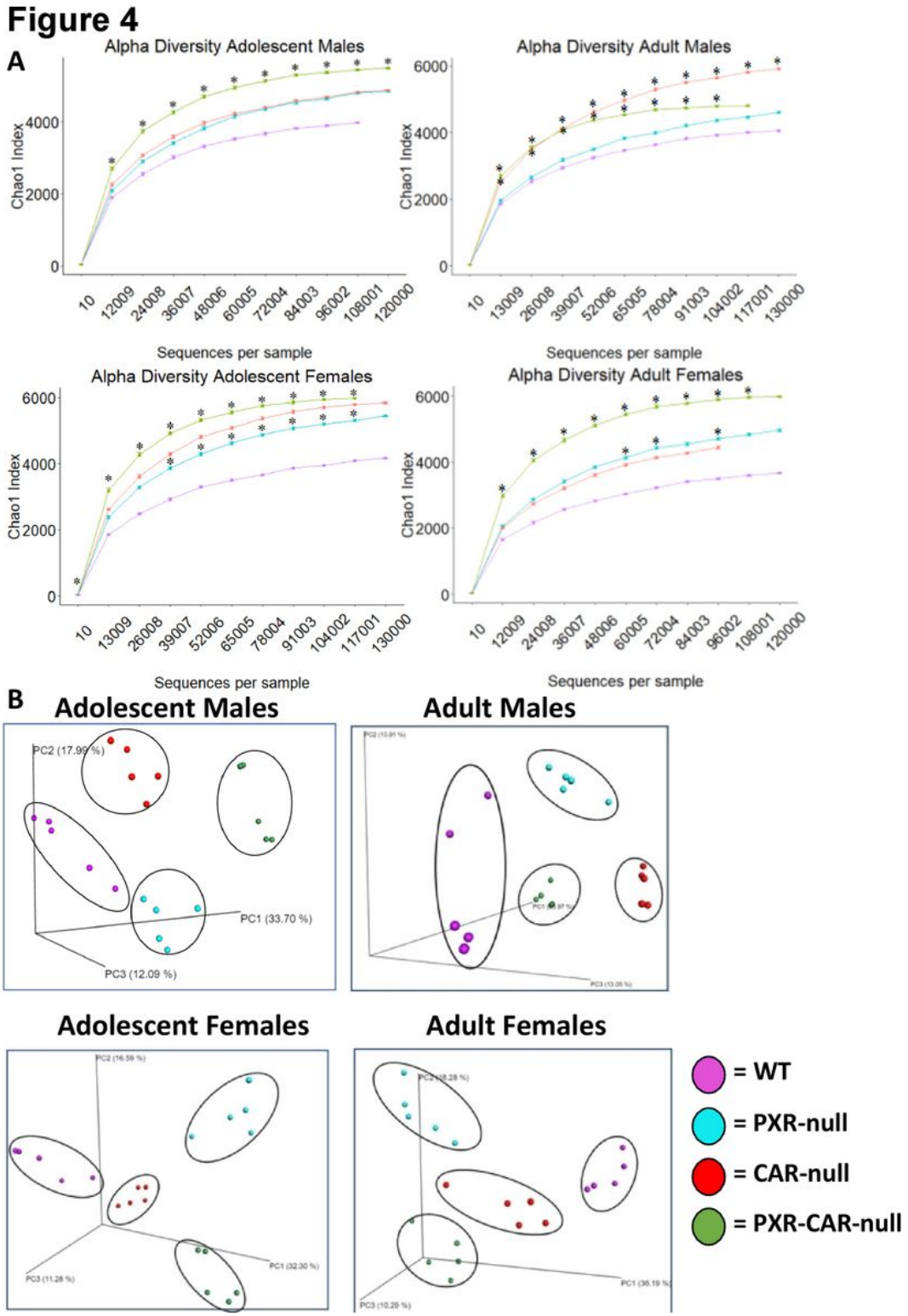

Figure 4

Alpha and beta diversities of WT, PXR-null, CAR-null, and PXR-CAR-null mice. A. Alpha diversity of gut microbiota within WT, PXR-null, CAR-null, and PXR-CAR-null mice. Line plots are generated using the R

package ggplot. Asterisks represent statistically significant differences compared to WT mice (one-way ANOVA followed by Duncan's post hoc test, $p < 0.05$). B. Principal components analysis (PCA) plots showing the beta diversities of adolescent male, adult male, adolescent female, and adult female WT, PXR-null, CAR-null, and PXR-CAR-null mice.

Figure 5

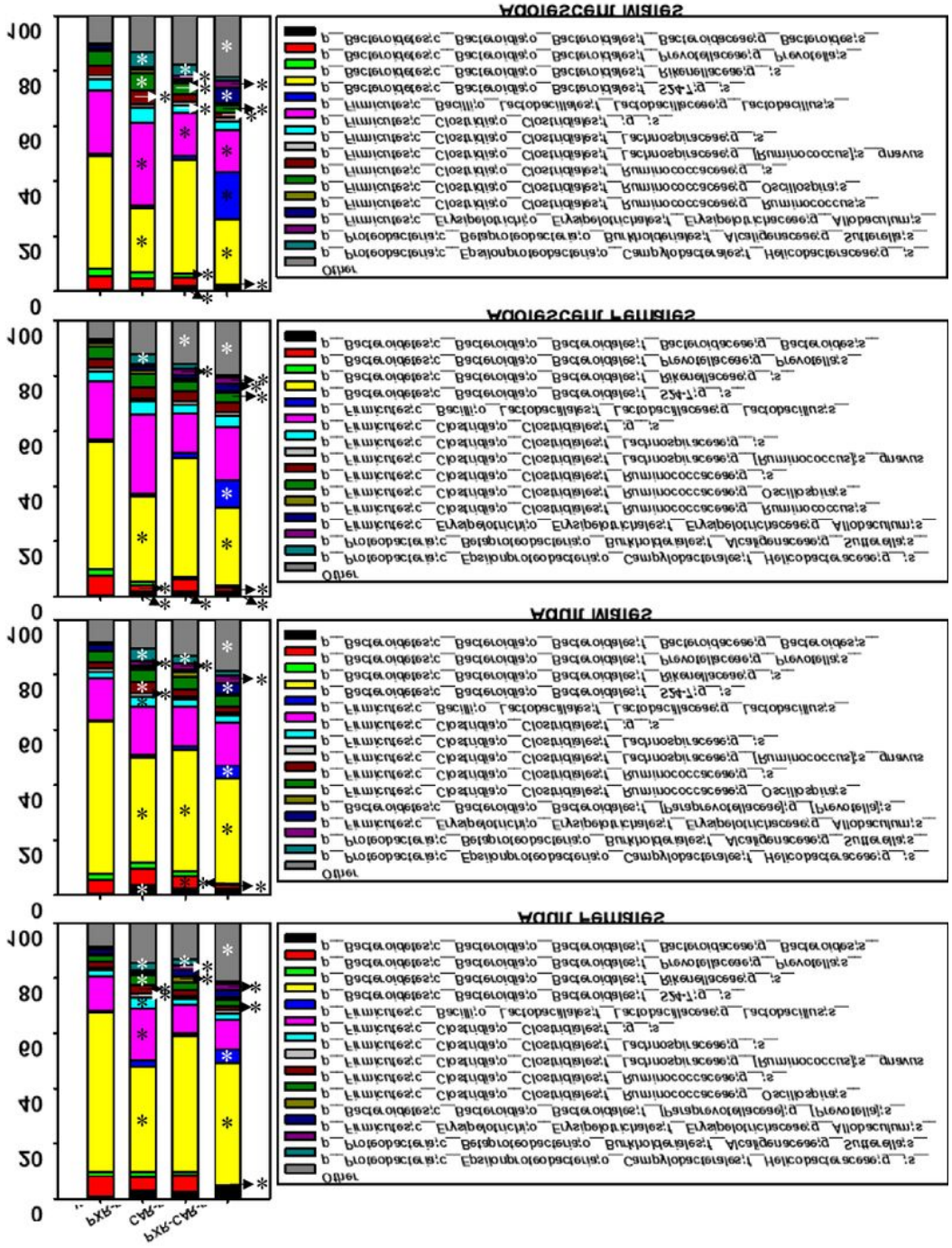

Figure 5

Percentage OTUs of the fecal microbiome among WT, PXR-null, CAR-null, and PXR-CAR-null mice. Stacked bar chart illustrates the percentage of differentially regulated taxa in fecal samples in WT, PXR-null, CAR-null, and PXR-CAR-null male and female, adolescent and adult mice. The top 14 differentially abundant taxa in each group were plotted and all other detected taxa were summed together to form the category labeled as “Other”. Asterisks represent statistically significant differences compared to WT mice (one-way ANOVA followed by Duncan’s post hoc test, $p < 0.05$).

Figure 6

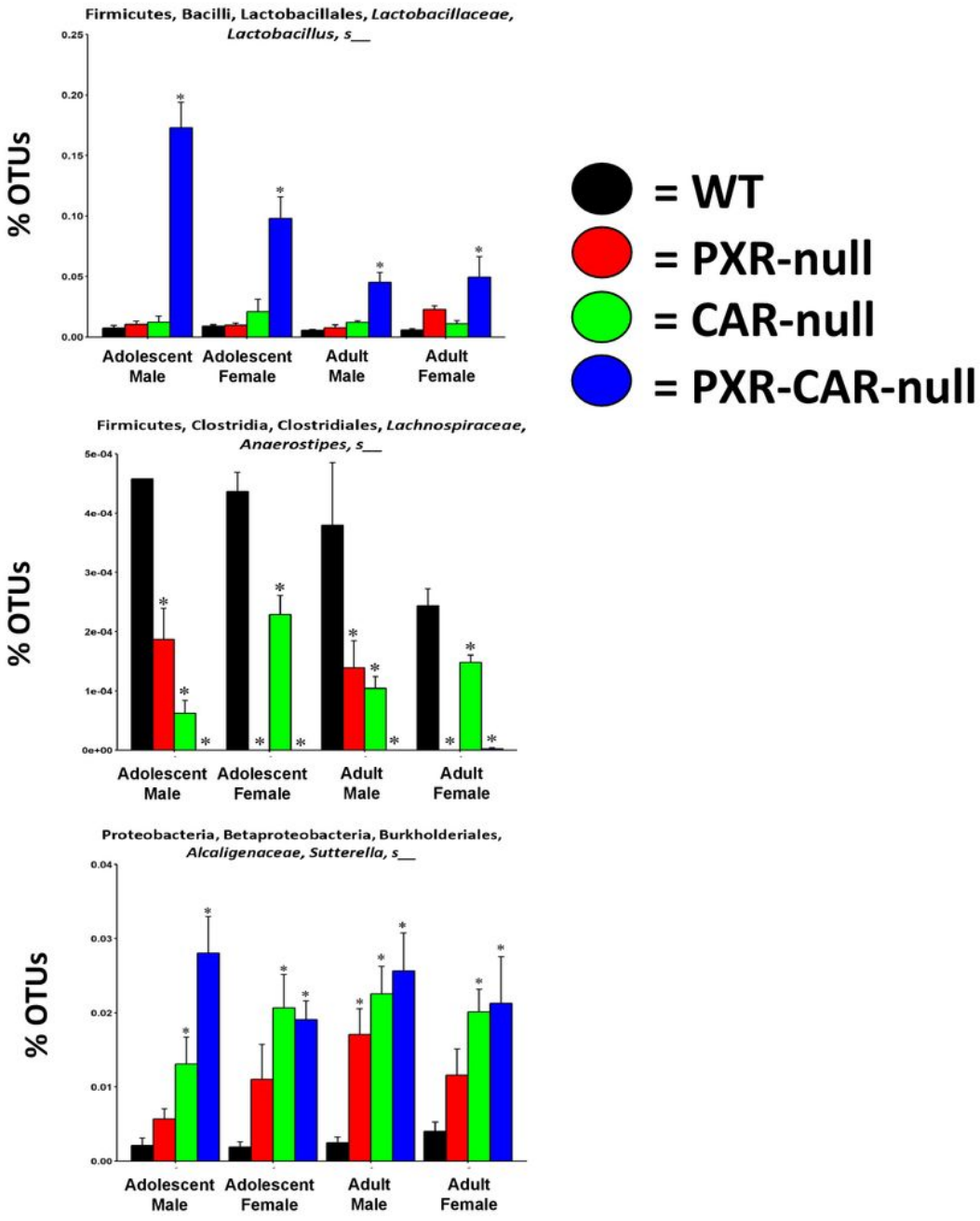

Figure 6

Percentage OTUs of Lactobacillus sp., Anaerostipes sp., and Sutterella sp. Individual bar plots of Lactobacillus sp., Anaerostipes sp., and Sutterella sp., are generated by the R package ggplot2. Asterisks represent statistically significant differences compared to WT mice (one-way ANOVA followed by Duncan's post hoc test, $p < 0.05$).

Figure 7

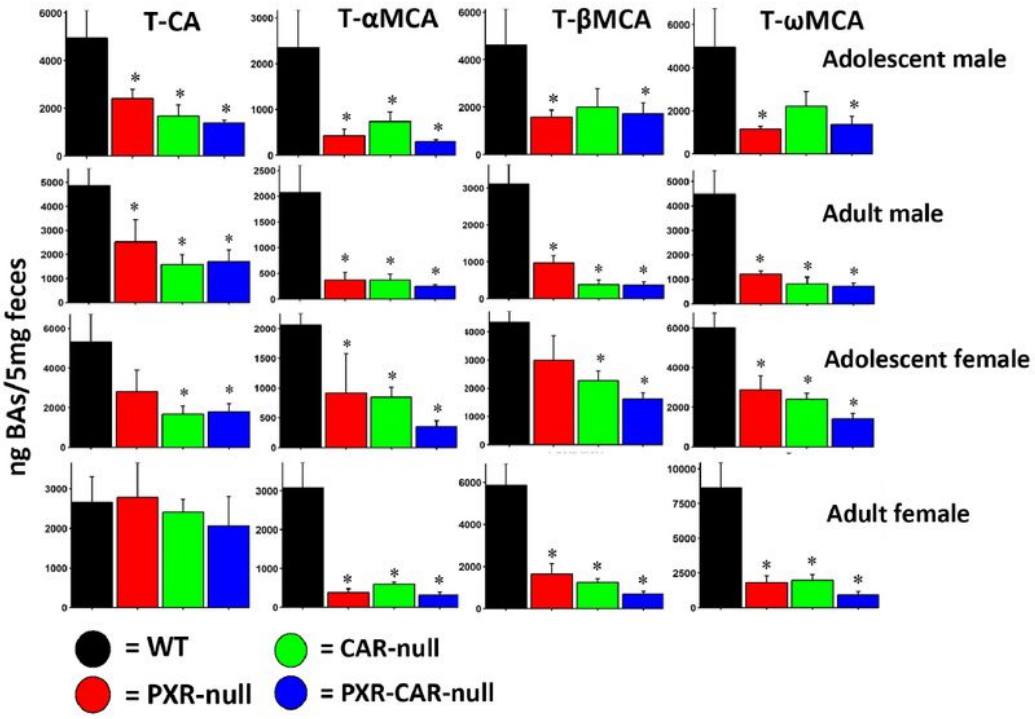

Figure 7

BA concentrations in WT, PXR-null, CAR-null, and PXR-CAR-null mice. Fecal BA concentrations (ng/mL) were quantified by LC-MS/MS as described in MATERIALS AND METHODS. Asterisks represent statistically significant differences compared to WT mice (one-way ANOVA followed by Duncan's post hoc test, $p < 0.05$).

Figure 8

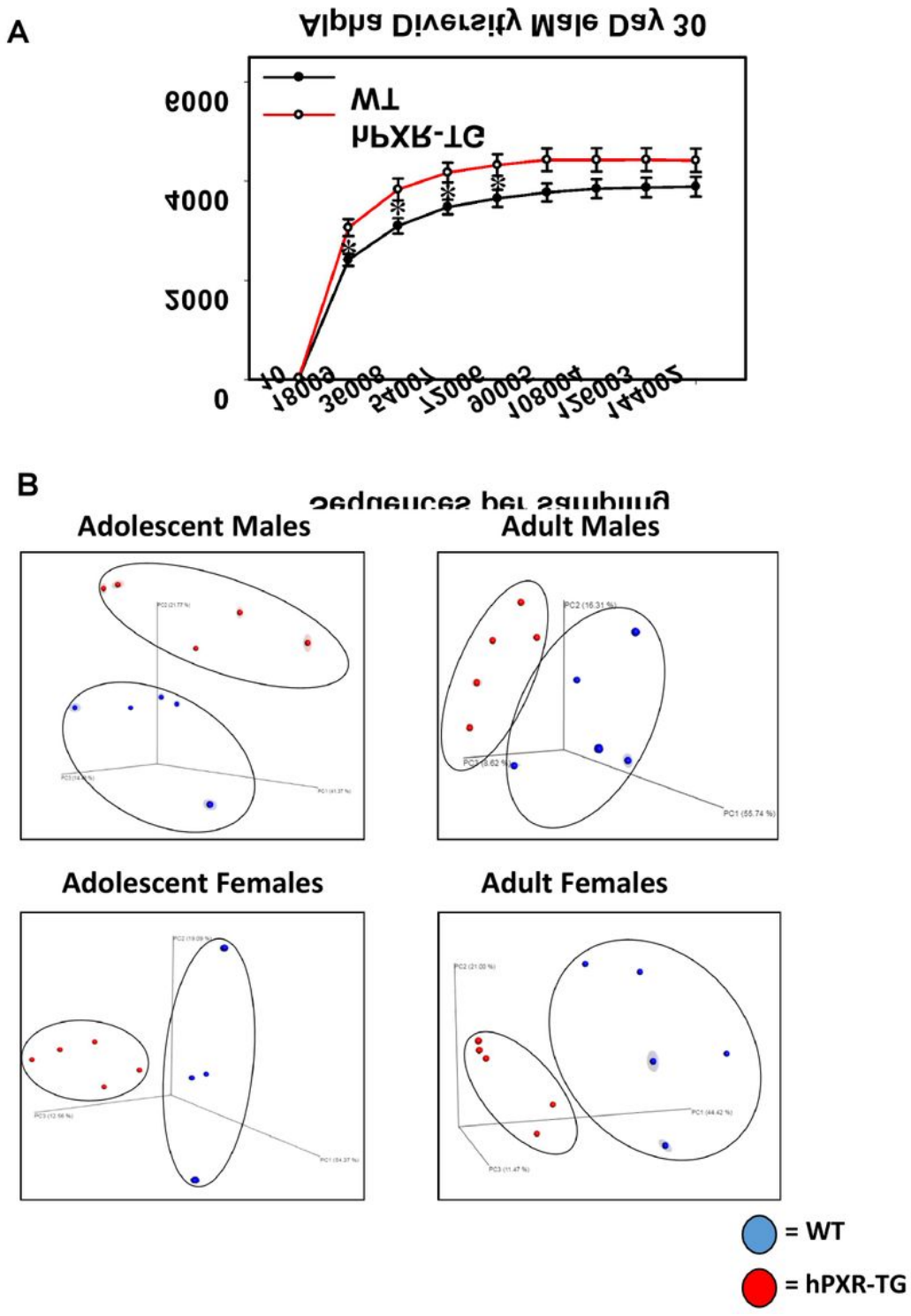

Figure 8

Alpha and beta diversities of WT and hPXR-TG mice. A. Alpha diversity of gut microbiota within WT and hPXR-TG FVB/NJ adolescent male mice. Line plots were generated using SigmaPlot. Asterisks represent statistically significant differences compared to WT mice (t-test, $p < 0.05$). B. Principal components analysis (PCA) plots showing the beta diversities of adolescent male, adult male, adolescent female, and adult female WT and hPXR-TG mice.

Figure 9

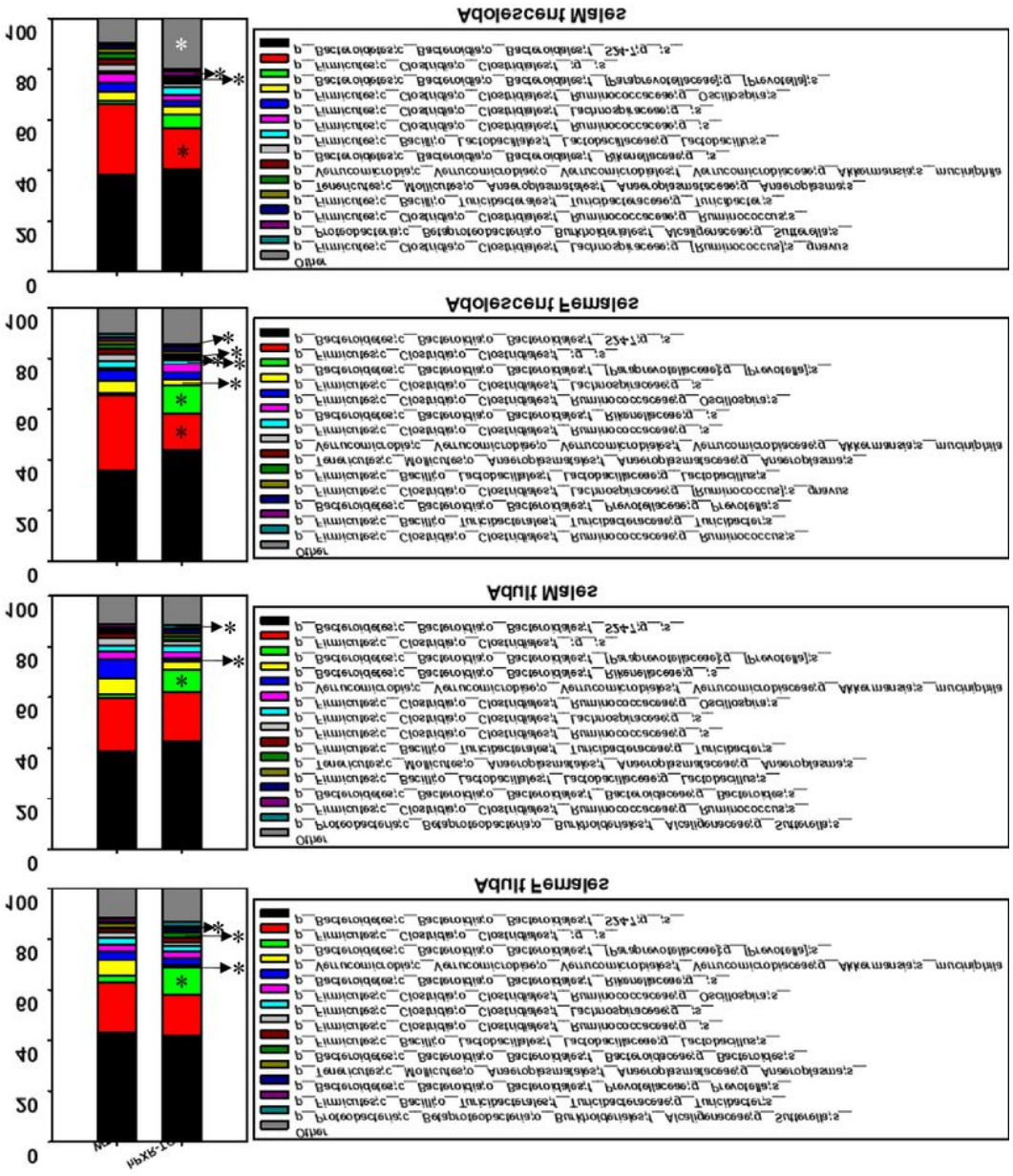

Figure 9

Percentage OTUs of WT and hPXR-TG mice. Stacked bar chart illustrating the percentage of differentially regulated taxa in fecal samples in WT and hPXR-TG male and female, adolescent and adult mice. The top 14 differentially abundant taxa in each group were plotted and all other detected taxa were summed together to form the Other category. Asterisks represent statistically significant differences compared to WT mice (t-test, $p < 0.05$).

Figure 10

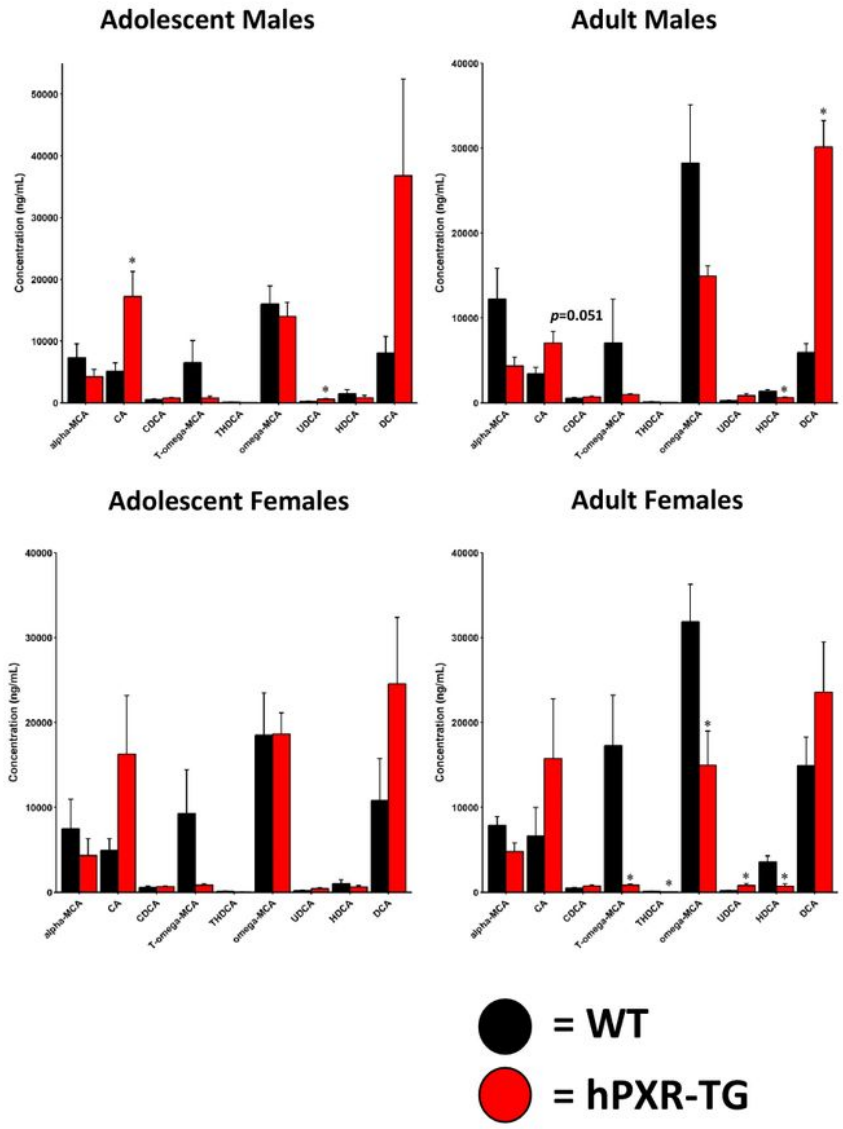

Figure 10

BA concentrations in WT and hPXR-TG FVB/NJ mice. Bar plots of BA concentrations (ng/mL) in WT and hPXR-TG mice as generated by the R package ggplot2. BAs were quantified by LC-MS/MS as described in MATERIALS AND METHODS. Asterisks represent statistically significant differences compared to WT mice (t-test, $p < 0.05$).

Figure 11

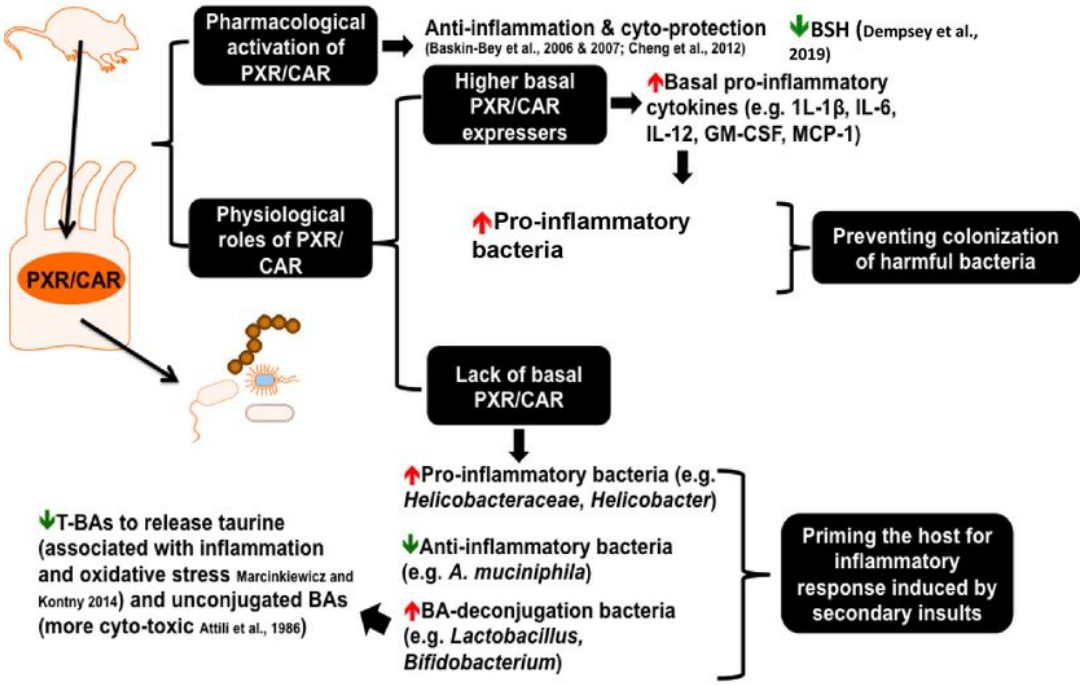

Figure 11

A diagram illustrating the key findings of the study. There is a bivalent hormetic relationship between PXR/CAR levels and the microbial richness, and PXR/CAR interacts with the gut microbiome to modulate immune surveillance and BA metabolism of the host.

Supplementary Files

This is a list of supplementary files associated with this preprint. Click to download.

- GenotypeSupplementalFiguresMLFinal.pptx
- SupplementaryFigureLegendsMLFinal.docx